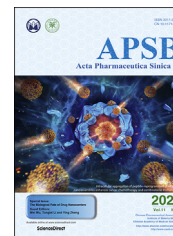




Chinese Pharmaceutical Association
Institute of Materia Medica, Chinese Academy of Medical Sciences

Acta Pharmaceutica Sinica B

www.elsevier.com/locate/apsb
www.sciencedirect.com



REVIEW

Exploration and insights into the cellular internalization and intracellular fate of amphiphilic polymeric nanocarriers



Samrat Mazumdar, Deepak Chitkara, Anupama Mittal*

Department of Pharmacy, Birla Institute of Technology and Science (BITS-PILANI), Pilani, Rajasthan 333031, India

Received 19 October 2020; received in revised form 20 December 2020; accepted 18 January 2021

KEY WORDS

Amphiphilic;
Copolymer;
Nanoparticles;
Internalization;
Intracellular fate

Abstract The beneficial or deleterious effects of nanomedicines emerge from their complex interactions with intracellular pathways and their subcellular fate. Moreover, the dynamic nature of plasma membrane accounts for the movement of these nanocarriers within the cell towards different organelles thereby not only influencing their pharmacokinetic and pharmacodynamic properties but also bioavailability, therapeutic efficacy and toxicity. Therefore, an in-depth understanding of underlying parameters controlling nanocarrier endocytosis and intracellular fate is essential. In order to direct nanoparticles towards specific sub-cellular organelles the physicochemical attributes of nanocarriers can be manipulated. These include particle size, shape and surface charge/chemistry. Restricting the particle size of nanocarriers below 200 nm contributes to internalization *via* clathrin and caveolae mediated pathways. Similarly, a moderate negative surface potential confers endolysosomal escape and targeting towards mitochondria, endoplasmic reticulum (ER) and Golgi. This review aims to provide an insight into these physicochemical attributes of nanocarriers fabricated using amphiphilic graft copolymers affecting cellular internalization. Fundamental principles understood from experimental studies have been extrapolated to draw a general conclusion for the designing of optimized nanoparticulate drug delivery systems and enhanced intracellular uptake *via* specific endocytic pathway.

Abbreviations: AR, aspect ratio; Cav-1, caveolin-1; CCP, clathrin coated pits; Cy, cyanine; DOX, doxorubicin; ER, endoplasmic reticulum; FITC, fluorescein isothiocyanate; HER-2, human epidermal growth factor receptor 2; IL-2, interleukin; mPEG, methoxy poly(ethylene glycol); RBITC, rhodamine B isothiocyanate; RES, reticuloendothelial system; R_{max} , minimum size threshold value; R_{min} , maximum size threshold value; SEM, scanning electron microscopy; SR & LR, short rod and long rod; TEM, transmission electron microscopy.

*Corresponding author. Tel.: +91 1596 515708.

E-mail address: anupama.mittal@pilani.bits-pilani.ac.in (Anupama Mittal).

Peer review under the responsibility of Chinese Pharmaceutical Association and Institute of Materia Medica, Chinese Academy of Medical Sciences.

<https://doi.org/10.1016/j.apsb.2021.02.019>

2211-3835 © 2021 Chinese Pharmaceutical Association and Institute of Materia Medica, Chinese Academy of Medical Sciences. Production and hosting by Elsevier B.V. This is an open access article under the CC BY-NC-ND license (<http://creativecommons.org/licenses/by-nc-nd/4.0/>).

1. Introduction

The ability to specifically and safely deliver drug molecules to the selected cell types at therapeutically effective concentration invokes a major challenge in drug delivery. One of the possible approaches to ensure safety, specificity and efficacy of drug molecules is the use of nanomedicines/nanoparticulate agents^{1,2}. The major goals of nanomedicine development includes creation of improved formulations with targeting ability and controlled drug release along with reduced toxicity and ability to bypass the biological barriers and reach the target site³. In order to accomplish these goals, nanomedicines must navigate through various endocytic pathways. Nanoparticles tend to undergo internalization predominantly *via* clathrin mediated endocytosis, caveolae mediated endocytosis or in certain cases *via* macropinocytosis⁴. The interaction of nanoparticles with cell membrane plays a crucial role in endocytosis and intracellular trafficking. This interaction is highly dependent on a myriad of factors including particle size, shape, surface charge, lipophilicity, nature of nanocarrier and cell involved in internalization⁵. Computational studies have revealed that endocytosis of nanoparticles occurs through membrane-particle adhesion followed by elastic deformation of the cell membrane and receptor diffusion to the surface of the membrane⁶, all these processes are highly dependent on the above mentioned factors. Therefore, designing an effective nanomedicine involves a comprehensive understanding of endocytosis and intracellular trafficking.

1.1. Endocytosis and intracellular trafficking

Endocytosis is responsible for internalization of particles from extracellular environment along with mediating various physiological and biochemical processes involving removal of cell debris generated from apoptosis, cell motility, immune surveillance, regulation of cell surface receptors and transporters, membrane remodelling, neurotransmission and intra and intercellular communications⁷. The regulation of endocytosis and intracellular trafficking is modulated by a host of associated proteins including coat proteins, adaptors, retrieval proteins and scission proteins along with Rab GTPases and soluble *N*-ethylmaleimide sensitive factor attachment protein receptor (SNARE)^{8,9}. Endocytosis is a type of active transport process which is highly beneficial for nanomedicines as it can direct the particles into cells¹⁰, while facilitated diffusion is a type of passive transport which aids in the transport of molecules across the membrane *via* specialized transport proteins. Further, particles bound to the cell membrane can bypass cytoplasmic barriers and reach into the perinuclear region¹¹. Subsequently, the risk of opsonisation is greatly reduced upon endocytosis and finally the acidic and neutral pH associated with clathrin and caveolae mediated entry respectively provides attractive options for tailor made drug delivery systems. Most nanocarriers gain entry into the cells by the process of endocytosis¹².

2. Endocytic mechanisms

Endocytosis can be classified into phagocytosis and pinocytosis. Phagocytosis is generally associated with the uptake of larger particles (>500 nm) and involves the participation of phagocytes which function to kill/remove foreign pathogen, dead cells and debris¹³. Following recognition *via* circulating phagocytes in the blood and tissues, nanoparticles get attached to the receptors present on the surface of phagocytes for further internalization¹⁴. Common phagocytic receptors involved in nanoparticle internalization include Toll-like receptors, mannose/lectin receptors and scavenger receptors¹⁵. The plasma membrane of phagocytes encloses nanoparticles within cup-shaped structure and later undergo fusion to form phagosomes. Subsequently, phagosomes fuse with lysosomes and undergo acidic degradation¹⁶. Pinocytosis can be further classified into clathrin mediated endocytosis (CME) and caveolae mediated endocytosis as depicted in Fig. 1.

2.1. Clathrin mediated endocytosis (CME)

CME is a fundamental process which serves to internalize molecules/cargo into the cell interior. The interactions occurring between the adaptor proteins and clathrin associated sorting proteins form coated pits along the plasma membrane which undergo disassembly *via* dynamin to form ~100 nm coated vesicles (CCV)¹⁷; subsequently, these vesicles are trafficked into early endosomes and subjected to degradation. The internalization of nanoparticles with particles size <200 nm bearing positive surface charge (>+10 mV) usually proceeds rapidly *via* CME⁴. Further, various molecules, growth factors and receptors including iron, transferrin, low-density lipoprotein receptor (LDLR) and epidermal growth factor receptor (EGFR) undergo CME providing opportunities for targeted therapy¹⁸. Recycling of molecules provides avenues to reverse cancer drug resistance of drug molecules by using pH triggered/responsive delivery systems, lysosomotropic agents and conjugates¹⁹. Additionally, disease states which are associated with lysosomes including lysosomal storage disease (LSD) and Alzheimer's could also highly benefit from direct intracellular entry of nanoparticles into lysosomes *via* CME²⁰.

2.2. Caveolae mediated endocytosis

Caveolae are characterized by non-planar lipid rafts that aid in cell signalling, vesicular transport and lipid regulation. The major integral protein associated with caveolae mediated endocytosis is caveolin (Cav-1), which triggers invagination of plasma membrane and formation of vesicles²¹. Structural investigations using high resolution electron microscopy revealed that caveolae are ~50–80 nm flask shaped membrane invaginations with an observable coating less prominent in comparison to clathrin coat. Further, caveolae are associated with constant shape and membrane curvature at the surface while CCV's undergoes dynamic remodelling²². Smaller nanoparticles <50 nm with surface charge

(between +15 to -15 mV) undergo caveolae mediated endocytosis. Additionally, targeted delivery of albumin, folic acid, oligonucleotide, HER2, TAT peptide and integrin based nanoparticles occurs predominantly through caveolae mediated uptake²³. Several marketed formulations of chemotherapeutic drugs including Doxil® and Ambraxane® have also been found to undergo internalization by caveolae mediated endocytosis²⁴. The major advantage associated with caveolae mediated pathway lies in its ability to avoid lysosomal degradation. During transient interaction with endosomes, the caveosome maintains its integrity without disassembly of caveolar coat and thus bypasses the lysosomes leading to efficient perinuclear trafficking into nucleus, Golgi and endoplasmic reticulum (ER)²⁵.

2.3. Macropinocytosis

It is involved in the acquisition of nutrients²⁶, immune surveillance and pathologies particularly cancer and viral²⁷. It is initiated by an actin driven extension of plasma membrane ruffles which result in the formation of large cup shaped endosomes termed

macropinosomes²⁸. These micrometer sized macropinosomes (0.2–5 μm) make it ideal for the uptake of macromolecules, large nanoparticles (>250 nm) and microbial pathogens. Subsequently, interaction with various organelles following membrane fusion and fission leads to the creation of acidic, tubular and mature structures termed macropino-lysosome²⁹. Nanoparticles or molecules in the extracellular fluid are encapsulated within macropinosomes by non-specific extracellular fluid uptake. While, the residual undigested particles are cleared *via* exocytic vesicles. Various therapeutic cargoes including lipid nanoparticles and lipoprotein based vehicles which target hepatocytes and nucleic acid aptamers also utilize macropinocytosis for efficient endocytosis³⁰. Further, the role of macropinocytosis in immune function is more pronounced; antigen processing cells (APC) commonly employ macropinocytosis for antigen presentation to T lymphocytes³¹.

The internalization of nanoparticles *via* specific endocytic pathway requires uniform size, shape and surface which can be achieved by PRINT technique³². Direct penetration of nanoparticles within the cells can be achieved by various artificial techniques including transmembrane penetration³³, electroporation³⁴ and cytoplasmic microinjection³⁵.

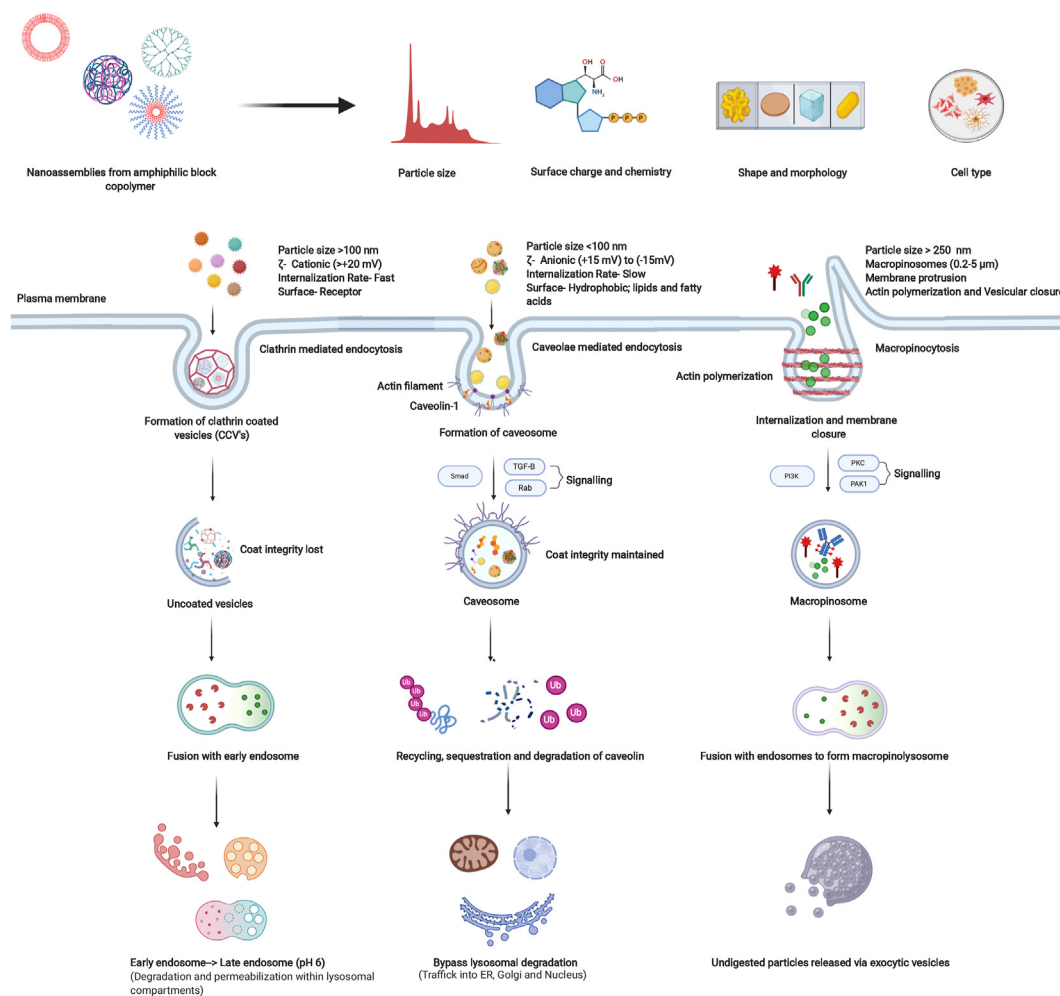


Figure 1 Schematic representation of endocytic pathways involved in the internalization of amphiphilic copolymers and the associated factors modulating their uptake pathways and intracellular fate.

Table 1 List of the most commonly used endocytic inhibitors along with their mechanisms.

Inhibitor	Endocytosis pathway	Mechanism	Ref.
Sucrose	Clathrin mediated endocytosis	Entrap clathrin within microcages	140
Potassium depletion	Clathrin mediated endocytosis	Removal of plasma membrane associated lattices	141
Cytosol acidification	Clathrin mediated endocytosis	Prevents budding off clathrin coated pits	142
Chloroquine	Clathrin mediated endocytosis	Alters the functioning of clathrin coated vesicles	143
Phenothiazines	Clathrin mediated endocytosis	Inhibits formation of clathrin coated vesicles	144
Chlorpromazine	Clathrin mediated endocytosis	Translocation of clathrin and AP2 from surface to endosomes	145
Phenylarsine oxide	Clathrin mediated endocytosis	Possibly tyrosine phosphate inhibitor	146
Monodansylcadaverine (MDC)	Clathrin mediated endocytosis	Stabilization of coated pits	147
Genistein	Caveolin mediated endocytosis	Tyrosine kinase inhibitor	148
Filipin	Caveolin mediated endocytosis, lipid raft	Binds to membrane cholesterol	149
Methyl- <i>b</i> -cyclodextrin	Caveolin mediated endocytosis, lipid raft	Depletion of cholesterol forming inclusion complex	150
Nystatin	Caveolin mediated endocytosis, lipid raft	Binds to cholesterol	149
Amiloride	Macropinocytosis	Lowers pH and prevents signalling	151
Cytochalasin D	Macropinocytosis	Disruption of actin filaments	152
Pitstop2	Clathrin mediated endocytosis	Inhibition of clathrin terminal domain and prevents coated pit formation	153
Concanavalin A	Clathrin mediated endocytosis	Mechanism unknown	154
LY294002	Macropinocytosis	Inhibition of PI3K	155
Rottlerin	Macropinocytosis	Selective inhibition of PKC-delta	156
Dynasore	Clathrin, caveolae mediated endocytosis	Blockage of dynamins	157
Monensin	Clathrin mediated endocytosis	Dysfunction of proton gradient	158

3. Amphiphilic copolymers

In recent years, research in the synthesis of amphiphilic block and graft copolymers for delivery of drugs has gained enormous interest. This is attributed to the unique properties imparted by two different parts/blocks varying in chemical nature in terms of hydrophilicity and hydrophobicity³⁶. Block copolymers can be defined as polymers comprising of linear arrangement of monomeric units with each block containing units derived from a characteristic monomeric species³⁵ while, amphiphilic block copolymers are formed by covalent binding of hydrophobic and hydrophilic blocks possessing single or multiple groups of hydrophilic/hydrophobic units. These amphiphilic copolymers offer several advantages over block copolymers like optimal drug solubilisation, particle size and stability during administration and transport³⁷. Moreover, due to the wide variability in chemical structure, these copolymers are also amenable to surface modification thus providing wider application in drug delivery. These amphiphilic copolymers can also form polymeric micelles in selective solvents at/above critical micelle concentration (CMC) which, can be used to efficiently encapsulate hydrophobic drugs and provide controlled release³⁸. Here, the hydrophilic portion provides opportunities for interaction with hydrophilic molecules including proteins and thus influences the pharmacokinetic properties. The physical and chemical properties of amphiphilic copolymers can be adjusted by varying the chain length, composition and architecture of copolymers³⁹. Further, modification of block characteristics enable good control over the copolymer properties including glass transition temperature (T_g), crystallinity, melting point and thermal degradation⁴⁰. However, the uptake mechanisms and intracellular trafficking routes of amphiphilic copolymeric nanocarriers are difficult to generalize as the physicochemical properties of polymer and cell type also

modulate uptake mechanisms. Amphiphilic block copolymers can assemble into diverse complex morphological structures including micelles, nanoparticles and polymerosomes with varied particle sizes, shapes and surface charge⁴¹. Further, amphiphilic block copolymers are also amenable to functionalization and have been explored extensively for drug delivery, targeting (peptide/ligand), and gene delivery^{42,43}. Nano-assemblies formed from amphiphilic copolymers not only encapsulate drugs but also interact with cells influencing pharmacokinetics and ultimately therapeutic efficiency. Thus, design aspects require a concrete understanding of the mechanisms associated with their internalization and fate within the cells. In comparison to inorganic nanoparticles, nanocarriers derived from amphiphilic copolymers offer greater scalability, biodegradability, drug loading and lower toxicity⁴⁴. Amphiphilic nanocarriers also exhibit lower *in-vitro* and *in-vivo* toxicities in comparison to lipidic counterparts following increased surface charge^{45,46}. Further, comparative studies indicated internalization of micelles *via* independent endocytic pathways as opposed to conventional endocytosis exhibited by liposomes⁴⁷. To understand the uptake mechanism and intracellular fate of nanocarriers different endocytic inhibitors are employed in endocytic inhibition studies and are represented in Table 1.

To the best of our knowledge, the factors affecting the internalization and intracellular fate of nanocarriers derived from amphiphilic copolymers have not been discussed till date^{48,49}. This review aims to provide an insight into the physicochemical attributes of nanocarriers affecting cellular internalization exemplified by specific studies on nanoformulations fabricated using amphiphilic copolymers. Additionally, the effect of polymeric structure including molecular weight, end group modification and lipophilicity in modulating the endocytic uptake has also been discussed along with other miscellaneous factors.

4. Factors affecting endocytosis of amphiphilic block copolymeric nanocarriers

4.1. Particle size

Size dependant internalization of nanocarriers has been explored extensively in various *in-vitro* cell culture studies as particle size is considered to be a key component in determination of endocytic pathways. Further, the circulation time, clearance and targeting of nanocarriers are also dependent on particle size⁵⁰. Recently Jiang et al.⁵¹ formulated self-assembled nanoparticles of cholesterol modified pullulan (CHSP) and studied their cellular uptake and intracellular fate in HepG2 cells. Fluorescent nanoparticles (FITC-CHSP) were formulated with particle size of 63.0 ± 1.9 nm and subjected to endocytosis inhibition studies in the presence of endocytic inhibitors. It was observed that uptake of CHSP nanoparticles was majorly through CME and macropinocytosis. However, caveolae mediated entry of nanoparticles was not observed which may be attributed to the absence of caveosomes in HepG2 cells. Further, to track the CHSP nanoparticles, various organelles including lysosomes, ER and Golgi apparatus were immunostained with antibodies, anti-LAMP2, anti-calnexin and anti-giantin respectively. Confocal imaging revealed that CHSP nanoparticles were confined to lysosomal compartment during the entire course of the study and did not localize into ER or Golgi confirming CME. Another study by Liu et al.⁵², involved the intracellular trafficking and cellular uptake of monomethoxy (polyethylene glycol)-poly(D,L-lactide-co-glycolide)-poly(L-lysine) (mPEG-PLGA-PLL) nanoparticles (PEAL) in HepG2, Huh7 and PLC cells. These nanoparticles were functionalized with 4-O- β -D-galactopyranosyl-D-gluconic acid (Gal) to form PEAL-Gal nanoparticles with particle size of 197.8 nm and uptake studies were performed in the presence of inhibitors. Quantitative analysis revealed primary role of CME and macropinocytosis during internalization of PEAL and PEAL-Gal nanoparticles. Further, colocalization assay in HepG2 cells using LysoTracker Red and FITC labelled PEAL and PEAL-Gal nanoparticles exhibited weak yellow fluorescence demonstrating that both PEAL and PEAL-Gal nanoparticles were not localized into lysosomal compartments suggesting early endosomal escape. However, higher fluorescence was observed in PLC cells following endocytosis of PEAL-Gal nanoparticles indicating susceptibility to lysosomal degradation depicted in Fig. 2.

Xin et al.⁵³ prepared rhodamine (RBITC) labelled angioprep-conjugated poly(ethylene glycol)-co-poly(ϵ -caprolactone) nanoparticles (ANG-PEP NPs) and investigated its uptake in BCEC cells in the presence of several endocytic inhibitors. The particle size of ANG-PEP NPs was found to be 92.7 ± 7.3 nm by DLS measurement. Results indicated that both CME and caveolae mediated endocytosis were involved in the uptake of ANG-PEP NPs by BCEC cells while macropinocytosis was not involved. Similarly, Nam et al.⁵⁴ studied the cellular uptake mechanism and intracellular fate of hydrophobically modified glycol chitosan nanoparticles (HGC; size 359 nm), to identify the uptake pathways responsible for internalization of HGC nanoparticles by HeLa cells. However, all the three pathways clathrin, caveolae and macropinocytosis were found to be responsible for its uptake and intracellular fate. It was thus concluded that more than one pathway contributed to endocytosis of HGC nanoparticles. Recent findings by Suen et al.⁵⁵ also suggested that variation in the particle size of nanoparticles contributed to internalization by different pathways. For this purpose, folate functionalized

mPEG-PCL nanoparticles with size ranging from 50 to 200 nm were incubated with ARPE-19 cells and uptake inhibition and kinetic studies were performed in the presence of endocytic inhibitors. It was observed that all the folate decorated nanoparticles (50, 120 and 200 nm) were primarily internalized by CME however, caveolae mediated pathway was also involved in the internalization of smaller nanoparticles (50 and 120 nm). Kinetic studies using mathematical models based on uptake rate and dissociation constant of folate decorated nanoparticles revealed that the rate of internalization of smallest nanoparticles was the fastest.

The effect of particle size on cellular internalization can be directly correlated to membrane wrapping which is in turn dependant on the deformation energy. The membrane deformation energy is constituted by bending and stretching energy in addition to deformation energy existing at the periphery of cell membrane. The complete internalization of spherical nanoparticles can be explained *via* the concept of R_{\min} and R_{\max} which are expressed mathematically⁵⁶. The threshold limit for internalization of nanoparticles is ~ 5 nm however, particles below the threshold limit can aggregate and undergo internalization. While, particles with diameter beyond threshold maxima (R_{\max}) do not undergo membrane wrapping due to existence of higher membrane tension and consequently fail to internalize efficiently. Based upon these and many similar literature reports, it is believed that endocytosis of particles ranging from 50 to 300 nm is usually supported by CCP and caveolae mediated pathways. Macropinocytosis has also been observed in certain cases however, both CME and caveolae mediated pathways are the predominant pathways by which nanoparticles undergo endocytosis based upon their particle size. Further, upon internalization by clathrin mediated pathway, nanoparticles are enclosed within the endosomes which undergo maturation to form late endosomes or vesicles and are then subjected to degradation by integration with lysosomal compartments/lysosomes.

Most of the studies in literature indicate that smaller nanoparticles internalize more efficiently in comparison to larger nanoparticles. Based upon thermodynamic studies and computational modelling, nanoparticles with size ranging from 30 to 50 nm exhibit favorable intracellular uptake and receptor mediated endocytosis⁵⁷. Particles with ~ 50 nm diameter, enter the cell as a single particle while smaller nanoparticles enter the cell following clustering. Further, for larger particles (>50 nm), wrapping is slower due to slower receptor diffusion kinetics leading to poor uptake⁵⁶. Polymeric nanoparticles with particle size 45 and 90 nm were formulated using tri-block copolymer, PEG 400-polyhexylene adipate-PEG 400 and subjected to endocytic inhibition studies in NR8383 and Caco-2 cells⁵⁸. Results indicated that both the nanoparticles were endocytosed by CME and caveolae mediated pathways however, almost 20% greater reduction in the uptake of smaller nanoparticles (45 nm) was seen in comparison to the larger polymeric nanoparticles (90 nm) following inhibition of clathrin and caveolae mediated pathways. Similarly, Niu et al.⁵⁹ investigated the uptake of amphiphilic aggregation-induced polyurethane nanoparticles (AIE-PU) flanked by PEG and PCL segments in primary human oral epithelial cells (HOEC). The average particle size of nanoparticles was found to be ~ 76 nm. CME and caveolae mediated pathways were mainly involved in the uptake of AIE-PU nanoparticles. Considering the uptake of ultra-small nanoparticles, these possess the ability to bypass conventional endocytic uptake to gain entry into the cells. The size of ultra-small nanoparticles lie between molecular

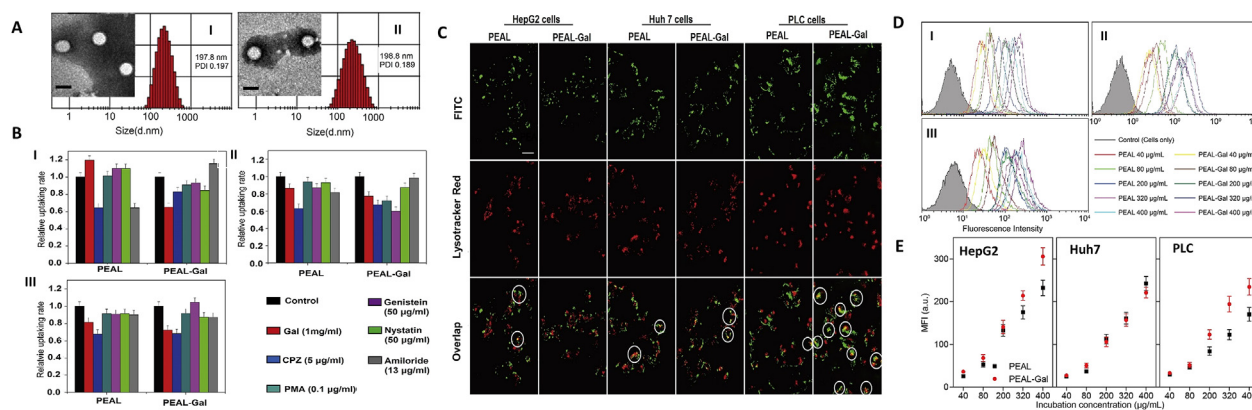


Figure 2 Size dependant internalization and intracellular trafficking of mPEG-PLGA-PLL (PEAL) and galactopyransoyl-*O*-gluconic acid modified PEAL (PEAL-Gal) nanoparticles for delivery into HepG2, Huh7 and PLC cells. (A) Particle size of PEAL nanoparticles (I) before and (II) after grafting of Gluconic acid (PEAL-Gal), (B) uptake of rhodamine loaded PEAL and PEAL-Gal (Rb/PEAL and Rb/PEAL-Gal) nanoparticles in (I) HepG2, (II) Huh7 and, (III) PLC cells in the presence of different uptake inhibitors; uptake was reduced in all the cells upon pretreatment with CPZ indicating CME. Uptake of PEAL nanoparticles by HepG2 cells also proceeded *via* macropinocytosis in addition to CME. (C) Colocalization assay using Lyotracker Red and FITC labelled PEAL and PEAL-Gal nanoparticles revealed higher yellow fluorescence in PEAL-Gal nanoparticles in PLC cells in comparison to PEAL nanoparticles in PLC, Huh 7 and HepG2 cells. Scale bar 20 μ m. (D) Flow cytometry images of (I) HepG2 (II) Huh7 and (III) PLC cells following incubation with various concentrations of Rb/PEAL and Rb/PEAL-Gal nanoparticles. (E) Quantitative data suggested increased uptake efficiency for PEAL-Gal nanoparticles in all the cell types—except Huh7 cells which exhibited higher uptake efficiency only at low concentration (≤ 80 μ g/mL). Reprinted with permission from Ref. 52. Copyright© 2014, Elsevier.

dispersion and large sized nanoparticles and exhibit unique properties in comparison to conventional nanoparticles. Verma et al.⁶⁰ synthesized ~ 6 nm amphiphilic nanoparticles coated with a shell of hydrophobic and anionic ligands. Uptake studies conducted at 4 $^{\circ}$ C indicated that the nanoparticles internalized into mouse dendritic cell clone DC 2.4 without the aid of active endocytosis and pinocytosis. Moreover, membrane poration was also not observed. A recent study reports the atomistic molecular dynamic simulations of amphiphilic monolayer protected nanoparticles comprising of binary compounds, 1-mercaptopundecanesulfonate (MUS) (anionic; hydrophilic sulfonate end group) and octanethiol (OT; purely hydrophobic); the particles so formed exhibited particle size ~ 4 nm and an amphiphilic anionic surface⁶¹. These ultra-small nanoparticles internalized in the cells by non-endocytic and non-disruptive pathways *via* ligand flipping due to reduced membrane bending and increased electrostatic interaction. Nanoparticles get adsorbed on the lipid bilayer of the cell membrane due to electrostatic interactions between ligand end group (charged) and lipid head groups (dipolar) following which, the nanoparticles diffuse into the lipid bilayer *via* protrusion. The charged endgroup undergoes sequential flipping until a stable thermodynamic configuration is attained and is translocated within the membrane completely. Ligand flipping avoids bilayer disruption which is otherwise linked to cytotoxicity thus enabling cytosolic drug delivery⁶².

4.2. Shape

Various simulation and experimental studies have highlighted the role of particle morphology in drug delivery and internalization although, there is no specific conclusion on the pathway selection based on particle shape⁶³. Nonetheless, particle shape and aspect ratio and their impact on plasma membrane wrapping upon endocytosis are crucial factors in determining the internalization rate as human cells are capable of internalizing both spherical and

non-spherical particles⁶⁴. It has been observed that viruses and bacteria with asymmetric morphologies are able to infect various cell types and get internalized into them⁶⁵. Their unique morphological features are inspiring the scientists to form nanostructures with different geometries which could enable rapid and enhanced uptake of the particles. In another study by Li et al.⁶⁶, bio-inspired spherical (S), short rod like (SR) and long rod like (LR) polymeric micelles of mPEG-PCL were formulated *via* self-assembly by adjusting the concentration of NaCl and loaded with DOX. The effect of shape of these micelles on internalization pathways was investigated in HeLa and HepG2 cells. Various inhibitors were selected to block the endocytic pathways, clathrin, caveolae and macropinocytosis. Uptake of S@DOX, SR@DOX and LR@DOX micelles in HeLa cells mainly occurred through CME and macropinocytosis. An interesting finding was that while caveolae mediated pathway showed negligible involvement in the uptake of micelles (S@DOX, SR@DOX and LR@DOX) in HeLa cells however, it was one of the contributing pathways responsible for uptake of rod shaped micelles in HepG2 cells. The difference in uptake between both cell lines could be attributed to poor expression of caveolin protein by HeLa cells. Specifically, spherical micelles (S@DOX) were internalized *via* CME in HepG2 cells. It was concluded that internalization mechanism also varied with micellar geometry/morphology since rod shaped micelles (SR@DOX and LR@DOX) were internalized by all internalization pathways while spherical micelles (S@DOX) were preferentially internalized by CME in both cell lines. Involvement of multiple pathways in the internalization of rod shaped micelles (SR@DOX and LR@DOX) in both the cells might be attributed to their multivalent interaction with cellular membrane resulting in stronger adhesion in comparison to spherical micelles possessing a single contact point. Findings by Hu et al.⁶⁷ also highlighted the role of particle morphology in cellular internalization. For this purpose, a polyprodrug amphiphile, comprising of PEG and polymerized block of reduction cleavable, disulphide bond linked

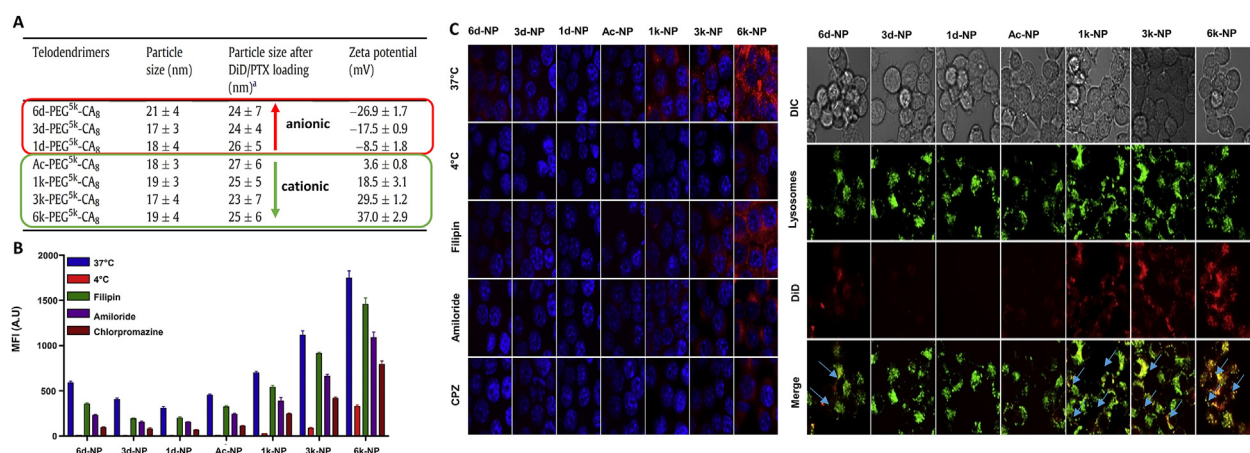


Figure 3 Shape dependent cellular internalization and subcellular localization of polyprodrug amphiphiles. (A) Illustration of self-assembly of PEG-*b*-PCTM amphiphiles (polymerized block of camptothecin prodrug monomer) into different nanostructures; spheres, smooth disks, large compound vesicles (LCV) and staggered lamellae. (B) Endocytic inhibition indicated that spherical nanoparticles were endocytosed by CME in both HepG2 and A549 cells whereas, clathrin and caveolae independent endocytosis both were associated with uptake of staggered lamellae and LCV. Furthermore, the uptake of smooth disk was dominated by clathrin and caveolae mediated endocytosis in both cells. (C) Subcellular localization of these nanostructures of different shapes in HepG2 and A549 cells following incubation for 4 h. Late endosomes/lysosomes were stained with Lysotracker red and mitochondria were stained with Mitotracker green. Colocalization analysis revealed that smooth disks, LCV and staggered lamellae were localized within the cytosol while spherical nanostructures remained entrapped within endolysosomes. Reprinted with permission from Ref. 67. Copyright© 2013, American Chemical Society.

camptothecin methacrylate monomer (CPTM) termed as PEG-PCPTM was used to form four types of self-assembled nanostructures including spheres, large compound vesicles (LCV), smooth disks and staggered lamellae. The cellular internalization and intracellular trafficking of nanostructures was also investigated in HepG2 and A549 cells using pharmacological inhibitors. Based on the results, it was concluded that spherical nanoparticles were endocytosed by CME in both cells whereas, clathrin and caveolae independent endocytosis were associated with uptake of staggered lamellae and LCV. Furthermore, the uptake of smooth disk was dominated by clathrin and caveolae mediated endocytosis in both cells. Colocalization analysis using Lysotracker Red revealed that staggered lamellae and LCV possessed high endosomal escape ability which was consistent with inhibition studies. On the other hand, both spherical and smooth disks were localized into the lysosomal compartment during initial incubation period (~1 h) however, smooth disks could efficiently escape from lysosomes in comparison to spherical nanoparticles upon extended incubation period (~4 h), this was validated using co-localization ratio of blue fluorescence from nanostructures with red fluorescence of Lysotracker Red depicted in Fig. 3.

Multivalency is a vital phenomenon which involves greater binding affinity between objects higher in order of magnitude in comparison to single-ligand receptor pair. Larger surface contact area in rods allows multivalent interactions with cell membrane thus initiating endocytosis wherein, two factors, adhesion force and bending resistance between particle and membrane plays a key role. Stronger adhesive forces allow complete membrane wrapping and endocytosis while stronger repulsive forces result in partial wrapping and no/incomplete endocytosis. Therefore, spherical micelles exhibited minimal interaction due to smaller contact area and lowest AR in comparison to SR and LR. Additionally, larger contact area is also correlated to larger size (~132 nm SR@DOX and ~202 nm LR@DOX) with AR being constant in both cases. Further, the internalization rates of high

AR nanoparticles (rods, disk) are highly dependent on entry angle as demonstrated by computational simulations by Deng et al.⁶⁸ wherein, their group developed stochastic model to study the clathrin mediated internalization of different ellipsoidal particles *viz.* spherical, oblate and prolate shaped ellipsoids with varying aspect ratios (AR) which is defined as ratio of length to width of a particle. This model is based on continuum and coarse-grained molecular dynamics (CGMD) and Monte Carlo simulations which involve membrane deformation and nanoparticle wrapping driven by the assembly of clathrin lattices which are activated in the presence of ligand receptor interaction. As transferrin receptors (Tf) are involved in CME, ligands specific to these Tf receptors were selected for determining the ligand receptor interaction parameter during simulation studies. Both the volume and ligand density for all particles were kept constant along with initial angles set at zero with respect to vector axis and a minimum of 5 simulations were performed for statistical significance. Results revealed three modes of entry to be existent during CME of spherical and ellipsoidal nanoparticles including tip-first (<15°), tilted entry (15–45°) and laying down modes (>45°). The three modes vary in the degree of rotation that the nanoparticles undergo during interaction with membrane based upon their curvature and contact angle. Both spherical and high AR oblate nanoparticles rotate (<10°) due to homogenous curvature of spherical nanoparticles and low curvature possessed by oblate nanoparticles. Thus these particles internalize by tip-first modes. While oblate nanoparticles with intermediate AR (1.17–1.47) undergo internalization by both tip-first and tilted entry modes. Compared to tip first entry, large degree of rotation (45°) during initial stages of interaction with the receptor indicates tilted entry. Subsequently, the rotation of particles facilitates bond formation on the curved edge of membrane leading to partial wrapping. Finally, the membrane is further bent towards the edges to accommodate the nanoparticles to form vesicular structures termed as clathrin coated pits (CCP) and thus internalized. No

“laying down” entry was observed for both spherical and oblate nanoparticles. In contrast, the clathrin mediated uptake of prolate ellipsoidal nanoparticles with AR (0.25–1.0) was also investigated using simulation techniques and same three entry modes were observed here also. The interaction of intermediate to high AR prolate nanoparticles (0.67–0.97) proceeded by tip first mode while lower AR prolate nanoparticles entered by laying down mode. Interestingly, moderate AR prolate nanoparticles (AR = 0.67) can be internalized by all three modes. This could be attributed to the rotation of the flat side and continuous interaction with membrane. Overall, prolate ellipsoidal nanoparticles rotate heavily in comparison to spherical and oblate nanoparticles due to high degree of curvature. Thus, the ability of nanoparticles to undergo endocytosis by any of three entry modes is important in drug delivery (transcellular) as the rate of internalization is dependant on the ligand receptor interaction. Lesser number of ligand-receptor bonds contribute to both increased internalization rate during endocytosis as well as a rapid particle release during exocytosis. Under, biological conditions the initial interaction between particle and membrane is almost random thus particles that can enter through all the modes possess higher endocytic probability. Further, it may be considered that shape dependant endocytosis of nanoparticles is highly correlated to their AR and extent of rotation during internalization. Another unique aspect of shape effect modulating the internalization pathway and *in-vivo* circulation of nanocarriers has been highlighted by the comparison between filament shaped cylindrical micelles termed filomicelles and their spherical counterparts⁶⁹. These self-assembled filomicelles were fabricated from a series of diblock copolymers comprising of PEG-polyethylene and PEG-polycaprolactone. Under static conditions involving incubation with A549 cells, it was observed that filomicelles tend to internalize into human lung epithelial cells *via* pinocytosis and traffick into perinuclear region. However, under dynamic and fluidic conditions, short and spherical particles were rapidly taken up by phagocytic cells while long filomicelles provided improved circulation time and were capable of bypassing phagocytic uptake. The experimental setup involved the utilization of flow chamber with immobilized phagocytes. Under dynamic conditions, the spherical particles interact and adhere with the immobilized phagocytes. While, the existence of strong hydrodynamic force between the filomicelles align themselves towards the direction of flow resulting in shorter contact time with immobilized phagocytes and improved circulation.

Based on literature reports, it has been observed that some of the nanoparticles and self-assembled micelles derived from amphiphilic block copolymers exhibit Janus like morphology during internalization into the cell through the phospholipidic membrane. Interaction of self-assembled micelles of mPEG-*b*-PCL block copolymer with a lipid bilayer model has been studied using coarse grained molecular dynamic simulations⁷⁰. It was observed that micelles derived from largely hydrophobic mPEG₅-*b*-PCL₉ copolymer undergo a gradual transition from its core-shell structure into a Janus-like morphology upon interaction with the lipid bilayer attributed to the exposure of mPEG block to the water outside lipid bilayer and polar head group region along with simultaneous interaction of hydrophobic PCL segments with the bilayer core. Similar rearrangement phenomenon termed as “snorkeling effect” was also observed for nanoparticles functionalized with hydrophobic segments possessing negatively charged hydrophilic groups^{71,72} and electroneutral PEG grafted hydrophobic nanoparticles⁷³. Simulations of amphiphilic Janus nanoparticles comprising of octadecanethiol conjugated cationic

silica nanoparticles with giant lipid vesicles (GLV; representing membrane model) revealed morphological deformation and disruption in the structural integrity of giant lipid vesicles⁷⁴. The binding of Janus nanoparticles induced significant membrane wrinkling with structural disorders attributed to the interaction of hydrophobic hemisphere with GLV. Further, membrane wrinkling arises when multiple particle-membrane interactions occur adjacent to each other leading to lateral compression of the membrane and wrinkling. Thus, amphiphilic Janus nanoparticles induce significant and efficient disruption of lipid bilayer in comparison to uniform amphiphilic particles. Wang et al.⁷⁵ have fabricated multicompartiment micelles (MCM) comprising of mPEG, PCL and poly(2-(perfluorobutyl) ethyl methacrylate) (PPFEMA) amphiphilic terpolymer with a particle size ~105 nm with adjustable Janus-cores. Cytocompatibility evaluation in 3T3 and THP-1 cells revealed that the micelles interacted with cell membrane *via* CME. Further, Brendel et al.⁷⁶ synthesized amphiphilic block copolymer comprising of PEG-pPGEA-pBA attached to asymmetric cyclic peptide (CP) conjugate, pBA-CP-pPGEA which self-assembled in aqueous solution to form Janus amphiphilic nanotubes termed as tubiosomes. The Alexa Fluor 488 labelled tubiosomes underwent accumulation into lysosomes following internalization into HEK293 cells as confirmed by confocal microscopy. It was further hypothesized that upon encapsulation into lysosomes the tubiosomes insert themselves in lipid bilayer of lysosomes. Interestingly, these tubiosomes also induced membrane disruption and generation of hydrophilic channels allowing cytosolic exchange and pH equilibration between cytosol and lysosomes. In yet another study, Cui et al.⁷⁷ designed bacillus shaped Janus like methotrexate (MTX) decorated mPEG-PLA nanoparticles termed MPEG-PLA-MTX NB. The MPEG-PLA-MTX NB presented weak anionic character (~–5 mV) with ~250 nm particle size. In order to elucidate the influence of shape, nanospheres with/without Janus faced function MPEG-PLA NS/MPEG-PLA-MTX NS were prepared and compared with MPEG-PLA-MTX NB. The cellular uptake of these nanoparticles labelled with Cy5.5 into HeLa cells indicated highest mean fluorescent intensity for MPEG-PLA-MTX NB signifying that bacillus shape improved endocytosis. Further, the internalization of Cy 5.5 labelled MPEG-PLA-MTX NB proceeded *via* receptor-mediated endocytosis/CME as confirmed by confocal microscopy. Two-dimensional nanoparticles with uniform shape, increased surface to volume ratio and surface charge provide enhanced biological functionality attributed to their internalization mechanisms. Evaluation of the endocytic mechanisms of FITC labelled PEGylated nanosheets in Saos-2, HepG2 and RAW 264.7 cells indicated that macropinocytosis was the major pathway responsible for the internalization of nanosheets in all the three cells⁷⁸. Additionally, CME was observed in HepG2 and RAW 264.7 cells. It has been observed that most 2D nanomaterials including nanosheets internalize into the cells *via* CME however, the internalization pathway involves a unique flat vesiculation event characterized by self-rotation and revolution during membrane wrapping⁷⁹.

4.3. Surface charge

It has been widely reported that cytomembrane is negatively charged however, nanoparticles can be cationic, anionic and neutral in nature based upon their surface charge. Cationic nanoparticles exhibit strong electrostatic interaction with cells and undergo rapid internalization. Further, cationic nanoparticles are

also susceptible to endosomal escape following internalization and display nuclear localization due to proton sponge effect. On the contrary, nanoparticles devoid of any surface charge are able to interact with cells *via* hydrophobic and hydrogen bonding interactions at physiological pH. Anionic nanoparticles are usually endocytosed due to the presence of positive sites on proteins present in the membrane. However, due to repulsive interaction with negatively charged membrane they undergo rapid RES uptake⁸⁰. Based on literature reports, it is usually observed that cationic nanoparticles enter the cell through multiple pathways including clathrin and caveolae mediated endocytosis, macropinocytosis and clathrin/caveolae-independent endocytosis. Anionic nanoparticles are usually internalized by caveolae mediated pathways while neutral particles do not exhibit specificity towards internalization routes⁸¹. Based on this, Frenkel et al.⁸² investigated the role of surface charge of nanoparticles in endocytosis in MDCK cells. For this purpose, PEG-D,L-poly lactide (PEG-PLA) copolymer was synthesized to formulate nanoparticles with different zeta-potential values, +32.8 mV (cationic NPs) and -26 mV (anionic NPs). Although, MDCK cells possess both apical plasma membrane and basolateral membrane, the various endocytic mechanisms including clathrin dependant and clathrin independent pathways exist only on the apical membrane. In order to observe clathrin mediated entry of nanoparticles at the apical membrane, dominant mutant polypeptides of dynamin and clathrin were expressed in MDCK cells (by transfecting them with recombinant adenoviruses encoding tagged dynamin (HA tag) and clathrin hub (T7 tag), both of which are capable of inhibiting clathrin mediated endocytosis. Upon incubation with nanoparticles, the endocytic mutants significantly reduced the uptake of cationic nanoparticles indicating that these nanoparticles were majorly internalized by CME. Inhibition in the uptake of anionic nanoparticles was lower indicating that they might also be internalized through other pathways like clathrin-dynamin independent pathways (macropinocytosis) in addition to CME highlighting the role of surface charge during internalization. Pang et al.⁸³, have investigated the intracellular delivery of biodegradable, cationic bovine serum albumin conjugated PEG-*b*-PCL nanoparticles (CBSA-PO). Coumarin-6 was used as a fluorescent molecule to probe the internalization of unmodified (PO) and cationic CBSA-PO nanoparticles possessing zeta potential values of -20.3 and + 9.5 mV respectively. The endocytosis inhibition studies performed in bEnd.3 cells revealed that the uptake of PO and CBSA-PO nanoparticles was primarily clathrin mediated however, uptake of cationic CBSA-PO nanoparticles in addition to CME, also involved caveolae mediated endocytosis. Similarly Xiao et al.⁸⁴ formulated PEG-oligocholic acid based micellar nanoparticles (NPs) and investigated the effect of surface charge on their cellular uptake. The distal ends of the PEG-oligocholic acid were derivatized with varying anionic and cationic units using aspartic acid and lysine respectively ($n = 0, 1, 3$ and 6). The micelles were based on self-assembly of linear-dendritic block copolymers (named as telodendrimer) comprising of PEG and dendritic cholic acids (CA) termed as PEG5k-CA8 where "8" indicates the number of CA subunits in the telodendrimer. A series of micelles were formed in aqueous medium with similar particle size but different surface charges. Seven types of PEG5k-CA8 NPs with various surface charge densities, including neutral acetylated NPs (Ac-NP), negatively charged NPs with one, three and six aspartic acid units (1d-NP, 3d-NP and 6d-NP) and positively charged NPs with lysine (1k-NP, 3k-NP and 6k-NP) were fabricated respectively. The zeta-potential of 6d-PEG5k-CA8, 3d-

PEG5k-CA8, 1d-PEG5k-CA8, Ac-PEG5k-CA8, 1k-PEG5k-CA8, 3k-PEG5k-CA8 and 6k-PEG5k-CA8 NPs was found to be -26.9, -17.5, -8.5, +3.6, +18.5, +29.5 and + 37 mV, respectively. The endocytic inhibition studies of these PEG5k-CA8 NPs in RAW 264.7 cells indicated the role of multiple pathways including CME and macropinocytosis during internalization of all the micelles. It was also observed that the uptake of anionic micelles (6d-PEG5k-CA8 and 3d-PEG5k-CA8) was more compromised in comparison to neutral and positively charged micelles upon treatment with various endocytic inhibitors specific to clathrin, caveolae and macropinocytotic uptake. In order to determine the effect of surface charge on intracellular fate in RAW 264.7 cells following endocytosis, colocalization assay was performed using LysoTracker Green and DiD labelled nanoparticles. Colocalization between lysosomal compartments and nanoparticles yielded merged images with yellow fluorescence. Results indicated the association of increased fluorescence with higher surface charge densities (both cationic and anionic) and majority of nanoparticles were entrapped within the lysosomes following internalization (Fig. 4).

Further, the role of surface charge on the internalization of polymeric nanoparticles (PNP) comprising of PEG₂₀₀₀-PHA-PEG₂₀₀₀ copolymer by NR8383 cells has been investigated by Bhattacharjee et al.⁸⁵ In this study, the terminal hydroxyl groups (PNP-OH) of PEG₂₀₀₀-PHA-PEG₂₀₀₀ were modified to introduce carboxylic acid (PNP-COOH) and ammonium groups (PNP-NH₂) with varying zeta-potential while the middle block poly(hexamethylene adipate) (PHA) in the triblock copolymer was labelled with fluorescent dye. The zeta-potential of PNP-OH, PNP-COOH and PNP-NH₂ was found to be -8, -25 and + 23 mV, respectively. NR8383 cells were pretreated with endocytic inhibitors in the presence of PNP nanoparticles. Results showed that uptake of positively charged PNP-NH₂ nanoparticles was mediated by CME. However, uptake of both PNP-OH and PNP-COOH nanoparticles indicated that caveolae mediated endocytosis was the preferred route for internalization. Thus, surface charge is a vital parameter which dictates the internalization of nanoparticles *via* endocytic pathways.

4.4. Cell type

In addition to the above mentioned factors, the effect or selection of cell type cannot be undermined. If a cell is devoid of a specific protein which is involved in a particular endocytic pathway then it cannot be adopted for the assessment of that specific internalization mechanism. Based on several studies, it has reported that HepG2 cells lack caveolin protein therefore, uptake of nanoparticles/nanocarriers by caveolin mediated pathways is not feasible in Hep G2 cells⁸⁶. Further, alteration in the environment, cell density and hormones might also influence the phenotype of cells and affect the endocytic internalization pathways⁴⁹. Interestingly, there exists a distinct variation between normal and tumour cells in terms of gene expression along with signalling and metabolic pathways. Recently, Liu et al.⁸⁷ have synthesized rhodamine conjugated chondroitin sulfate-graft-poly(ϵ -caprolactone) copolymer (Rh123-H-CP) which self-assembled into micelles in aqueous media. The endocytic inhibition studies were performed in CRL-5802 and H1299 lung carcinoma cells in the presence of inhibitors. Results revealed that both clathrin and caveolae mediated endocytosis were responsible for the internalization of Rh123-H-CP micelles in CRL-5802. However, caveolae mediated endocytosis was only observed during internalization of Rh123-H-CP micelles by H1299 cells. Further, Zhou et al.⁸⁸ have synthesized *N*-(2-hydroxypropyl) methacrylamide (HPMA) copolymers which were

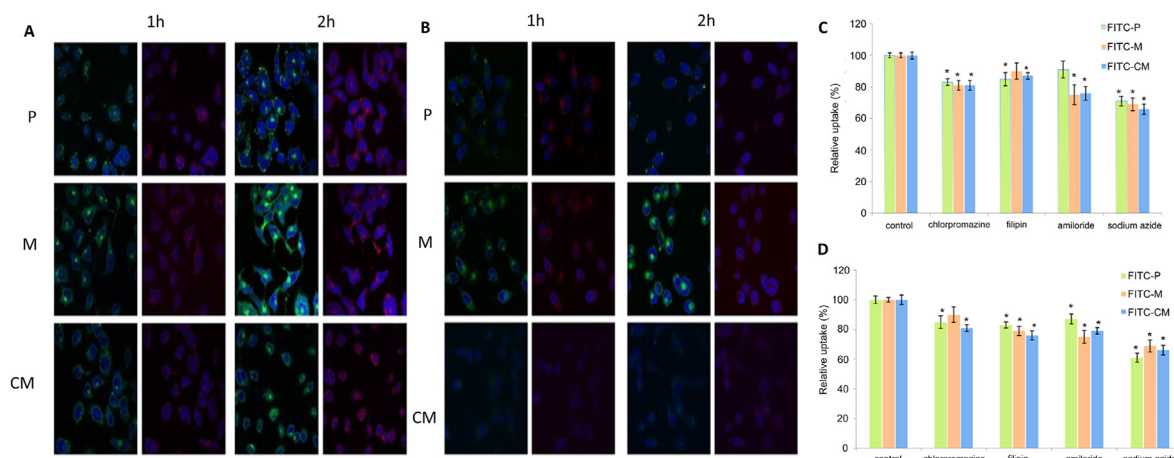


Figure 4 Influence of surface charge on cellular internalization of PEG-oligocholic acid dendrimers (PEG5K-CA8 NPs). The distal ends of PEG were functionalized with either anionic aspartic acid residues or cationic lysine residues ($n = 0, 1, 3, 6$). (A) The particle size of PEG5K-CA8 NPs remained uniform following functionalization however, increasing aspartic acid residues contributed to higher anionic character while lysine residues provided positive surface potential. (B) The uptake of PEG5K-CA8 NPs by RAW 264.7 murine cells following pretreatment with various endocytic inhibitors. Both macropinocytosis and caveolae mediated endocytosis were prominent for anionic PEG5K-CA8 NPs while both anionic and cationic PEG5K-CA8 NPs were also internalized by clathrin mediated pathways. (C) Confocal microscopic images of cellular uptake following incubation with DiD labelled PEG5K-CA8 NPs and pretreatment with endocytic inhibitors. Most of the inhibitors inhibited the uptake of nanoparticles to varying degree. Uptake was energy dependant process and underwent reduction at low temperature. (D) Colocalization assay using LysoTracker Green and DiD labelled PEG5K-CA8 NPs indicated that higher cationic character of PEG5K-CA8 NPs increased the internalization propensity by lysosomes represented by yellow fluorescence (indicated by arrows). Reprinted with permission from Ref. 84. Copyright© 2011, Elsevier.

conjugated to anti-cancer drug doxorubicin (DOX) and the hydrophobic phytosterol- β -sitosterol (SITO) *via* hydrazone linkages to form pHPMA-DOX-SITO copolymeric micelles. Subsequently, the internalization of these micelles by HepG2 and A549 cells was evaluated in the presence of inhibitors. Both caveolae and clathrin mediated endocytosis were involved in the intracellular uptake of pHPMA-DOX-SITO micelles in both the cells. However, macropinocytosis was involved during the uptake of micelles solely in A549 cells suggesting that endocytosis is cell type specific (Fig. 5). Similarly, Qiu et al.⁸⁹, have elucidated the endocytic mechanism of heparosan polysaccharide (hydrophilic) and cholesterol (hydrophobic) based micelles (KC) loaded with doxorubicin (DOX/KC micelles) in various cancer cells. The endocytic pathways were studied using A549, B16 and MGC80-3 cells in the presence of pharmacological inhibitors. Results indicated that CME and macropinocytosis was involved in the internalization of DOX/KC micelles by A549 and MGC80-3 cells respectively. While the existence of multiple endocytic pathways including clathrin, clathrin/caveolae independent endocytosis and macropinocytosis was confirmed during internalization of DOX/KC micelles by B16 cells. In another study, PEG-PLGA polymeric micelles were loaded with Nile red fluorescent dye and subjected to endocytic inhibition studies in Calu-3 and NCI-H441 cells using several inhibitors⁹⁰. Results indicated clathrin and caveolae dependant internalization of micelles in both the cells. However, micelles were internalized and translocated within Calu-3 cells more efficiently in comparison to NCI-H441 cells. This could be attributed to variation in source of cells wherein, Calu-3 cells were obtained from patient with lung adenocarcinoma while NCI-H441 cells were derived from a patient with papillary adenocarcinoma.

A closer examination into the factors affecting internalization and intracellular fate of nanocarriers have also revealed the uniqueness of cellular characteristics which is often disregarded.

Significant variations during uptake of nanoparticles is also attributed to cell sex (derived from male/female lineage), cell age and cell shape⁹¹. Recently, it has been reported that male derived cells exhibit greater uptake of nanoparticles in comparison to female derived cells. Possible explanation for this comes from an abundance of actin filaments in female derived cells which is correlated with increased cellular stiffness and altered membrane bending. Similarly, the effect of cell age on PEGylated nanoparticle uptake was investigated using young and senescent human fetal lung IMR90 fibroblast cells and human fetal colon CCD841CoN epithelial cells⁹². Induction of senescence was achieved by serial passaging, oxidative stress (in the presence of hydrogen peroxide) and DOX induced senescence. Results indicated significant reduction in energy dependent uptake in senescent cells in comparison to young cells due to mitochondrial deterioration and lowered ATP production. Further, down-regulation of amphiphysin-1 (involved in CME) and upregulated caveolin receptors were linked to defective receptor mediated endocytosis occurring in senescent cells. The nanoparticles were majorly internalized *via* CME following treatment with endocytic inhibitors specific to clathrin and caveolae mediated pathways in IMR90 fibroblast cells and human fetal colon CCD841CoN epithelial cells. Subsequently, lysosomal staining also indicated higher lysosomal content within senescent cells in comparison to young cells. Thus, cell age is yet another important factor which needs to be considered prior to internalization and intracellular targeting. The cellular uptake of nanoparticles is also strongly dependent on cell morphology which is seen to undergo a significant variation when the cells are grown on cell culture plates (2D) vs. native environment using 3-dimensional cell imprinted substrates⁹³. Results revealed that cells cultured on smooth substrates were capable of higher uptake due to greater exposure to cell media. However, the reduced availability of endocytic

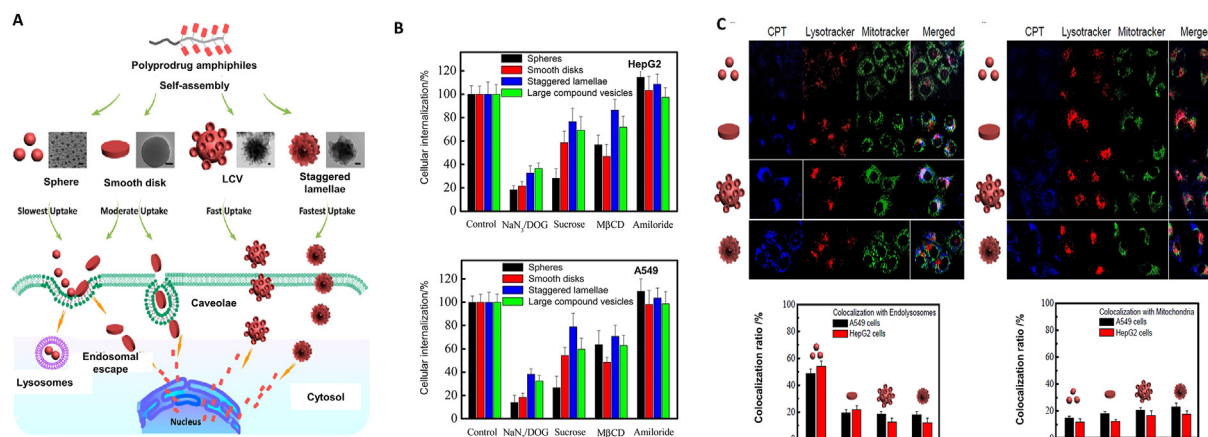


Figure 5 Effect of cell type on the internalization of *N*-(2-hydroxypropyl) methacrylamide (HPMA) copolymers in HepG2 and A549 cells. Uptake of FITC labelled pHPMA-DOX-SITO copolymer drug conjugates (P) which self-assembled to form pHPMA-DOX-SITO micelles (M) and pHPMA-DOX-SITO cross-linked micelles (CM) following treatment with glutaraldehyde. Qualitative uptake studies by confocal imaging in, (A) HepG2 and, (B) A549 cells following incubation for 1 and 2 h. Quantitative uptake studies by flow cytometry in, (C) HepG2 and, (D) A549 cells following pretreatment with inhibitors incubated for 2 h. 2 panels in each of (A) and (B) exhibit green signal of FITC-labelled copolymers while red signal reflects DOX. The uptake of copolymers was mediated by clathrin, caveolae and macropinocytosis in both cells. However, amiloride significantly inhibited uptake of pHPMA-DOX-SITO copolymers in A549 cells in comparison to HepG2 cells suggesting that endocytosis is cell type specific. Reprinted with permission from Ref. 88. Copyright© 2014, Elsevier.

receptors on cells grown on imprinted substrates led to early saturation in comparison to cells grown on smoother substrates thereby reducing the uptake potential of nanoparticles. From these studies, it is quite evident that sensitivity of cell lines for specific inhibitors is cell type dependent. Under *in-vivo* conditions it is imperative that endocytosis inhibitor selection and concentration levels needs careful consideration due to the existence of heterogeneous environment within the cells/tissues.

Few additional examples based on the affect of above discussed parameters on endocytosis and intracellular fate of nanocarriers have been summarized in Table 2.

4.5. Miscellaneous factors

4.5.1. Effect of pegylation

It has been widely reported that nanoparticles exhibit promising properties as therapeutic carriers which can efficiently deliver molecules including DNA, proteins and drugs into the cell. The surface of nanoparticles is often grafted with PEG for improved solubility, avoidance of aggregation and prevention of opsonization and rapid uptake by RES. However, existing reports also indicate that surface modification with PEG results in alteration of internalization pathways thus modulating intracellular fate as well. Additionally, variation in PEG chain length, molecular weight, layer thickness, density and conformation also contribute towards differential endocytic pathways^{39,94}. In a study conducted by Ibricevic et al.⁹⁵, PEGylated cationic shell-crosslinked-knedel-like nanoparticles (cSCKs) were prepared and evaluated for endocytic inhibition studies. The nanoparticles were assembled from poly(acrylamidoethylamine graft-poly(ethylene glycol))-block-polystyrene (PAEA-*g*-PEGb-PS) copolymer and both pegylated (cSCK-PEG) and non-pegylated (nonPEG cSCKs) nanoparticles were prepared with zeta-potential of +8.63 and +21.7 mV respectively. Endocytic uptake of cSCK-PEG and nonPEG cSCKs nanoparticles by MLE 12 cells was determined in the presence of inhibitors. Based on the results obtained, it was found that clathrin

mediated pathway was responsible for the uptake of nonPEG cSCKs nanoparticles. Subsequently, dynasore restricted the internalization of both cSCK-PEG and nonPEG cSCKs nanoparticles indicating the participation of dynamin dependant pathways as well. Thus, PEGylation of cSCKs led to altered entry mechanisms within the cells.

Similarly, Yang et al.⁹⁴ evaluated the impact of PEG chain length on the physical properties and bioactivity of PEGylated chitosan/siRNA nanoparticles. For this purpose, a series of chitosan PEG copolymers (CS-PEG2k, CS-PEG5k and CS-PEG10k) were synthesized with similar PEG mass content and varying molecular weight. The mechanism of endocytosis of non-pegylated chitosan copolymer (CS) and pegylated chitosan copolymer CS-PEG5k was evaluated in Hela cells using endocytic inhibitors. Non-PEGylated nanoparticles were internalized non-specifically by multiple pathways including clathrin, caveolae pathway and macropinocytosis. While, macropinocytosis and caveolae were the major pathways responsible for uptake of PEGylated nanoparticles. Thus, PEGylation caused a significant change in the endocytosis pathway of chitosan based nanoparticles. The overall study objective was based on effect of PEG chain length but specifically for endocytic studies, the effect of pegylation was explored.

Sant et al.³⁹ evaluated the cellular interaction of nanoparticles prepared from four different polymers, viz., poly(D,L-lactide) (PLA), poly(ethylene glycol)1%-graft-poly(D,L-lactide) (PEG1%-*g*-PLA), poly(ethylene glycol)5%-graft-poly(D,L-lactide) (PEG5%-*g*-PLA), and (poly(D,L-lactide)-block-poly(ethyleneglycol)-block-poly(D,L-lactide))_n copolymer (PLA-PEG-PLA)_n. The mean particle size of all these nanoparticles was found to be in the range of 180–192 nm. While zeta potential varied with increasing PEG content (PEG1%-*g*-PLA; $\zeta = -5.97$ mV), (PEG5%-*g*-PLA; $\zeta = -7.72$ mV), -2.5 mV for PLA nanoparticles and (PLA-PEG-PLA)_n nanoparticles exhibited zeta-potential of -22.72 mV. The endocytic inhibition studies of fluorescently labelled nanoparticles composed of these different polymers into RAW 264.7 cells were carried out.

Table 2 An overview of the factors influencing internalization and intracellular fate supported by experimental findings.

Parameter	Nanocarrier	Pathway	Remark	Ref.
Particle size	DOX loaded poly(<i>ε</i> -caprolactone)- <i>b</i> -poly(<i>N,N</i> -diethylaminoethyl methacrylate)- <i>r</i> poly(<i>N</i> -(3-sulfopropyl)- <i>N</i> -methacryloxyethyl- <i>N,N</i> ,diethylammonium betaine) (4sPCLDEAS) micelles	Clathrin, caveolae, macropinocytosis	Uptake of micelles with mean diameter 127 nm was 2.4, 1.2 and 1.2 folds higher in comparison to the micelles with particle size 366, 185 and 88 nm, respectively. Confocal microscopy indicated lysosomal localization.	159
	Insulin loaded poly(2-lactobionamidoethyl methacrylate-random-3-s-acrylamidophenylboronic acid) p(LAMA- <i>r</i> -AAPBA) nanoparticles	Clathrin and caveolae	Glycopolymer self-assembled into ~300 nm NPs. Compared to control (insulin alone), the uptake of FITC-insulin-loaded NPs exhibited higher fluorescent intensity indicating increased binding to cell surface and enhanced transport of insulin attributed to the presence of phenylboronic acid and physicochemical properties of NPs	160
	PTX loaded 2-deoxy-D-glucose functionalized PEG- <i>co</i> -poly (trimethylene carbonate) (PEG-PTMC) nanoparticles	Clathrin and caveolae	Clathrin and caveolae	Mean diameter of D-Glu NPs ~71 nm; compared to non-glucosylated NPs, significant amount of D-Glu NPs were internalized through CME and caveolae mediated endocytosis and localized into lysosomal compartment
Shape	PEG-1,3-bis(<i>p</i> -carboxyphenoxy) propane (CPP) and sebacic acid (SA) (PEG-CPP-SA) micelles	Clathrin, caveolae macropinocytosis	Uptake of polyanhydride micelles with different architectures indicated that spherical micelles were endocytosed by CME while, rod-like and comb-like micelles were internalized by macropinocytosis and caveolae mediated pathways.	162
	DOX loaded 1,2-distearyl- <i>sn</i> -glycero-3-phosphocholine (DSPC) and PEG5000-glyceryl distearate non-spherical particles	Non-clathrin and caveolae, clathrin, macropinocytosis	Non-spherical PEG-stabilized bilayer nanodisks. Internalization into cells mediated by energy-dependent endocytosis and uptake attributed to discoid shape, large surface area and high aspect ratio (AR = 12).	163
Surface charge and chemistry	Penetratin functionalized PEG-D,L-poly(lactide) (PEG-PLA) nanoparticles	Caveolae	Anionic NPs (−20.5 mV) internalized <i>via</i> caveolae. In addition to caveolae; Golgi, lysosomes and microtubules were also involved in cellular transport of cationic NPs which were formed <i>via</i> conjugation of penetratin onto the surface of anionic NPs (−4.42 mV). Energy-independent internalization was observed for cationic NPs due to translocation of Penetratin	164
	Oligoarginine modified PEG- <i>b</i> -poly(<i>ε</i> -caprolactone) (mPEG-PECL) nanoparticles	Clathrin and caveolae	Non-modified mPEG-PECL NPs exhibited negative zeta-potential (~−4 mV); surface modified NPs with 1-, 4- and 8-residues long oligoarginines termed as R1PECL, R4PECL and R8PECL with zeta-potential values +20, +30 and +40 mV. Clathrin involved in the uptake of mPECL and R1PECL NPs. Uptake of R4PECL and R8PECL NPs was mediated by caveolae endocytosis.	165
Cell type	CPT loaded chondroitin sulfate-graft-poly(<i>ε</i> -caprolactone) micelles	Clathrin and caveolae	Endocytic inhibition studies of rhodamine labelled micelles (Rh123-H-CP) revealed clathrin and caveolae mediated endocytosis for their internalization in CRL-5802 cells. However, caveolae mediated endocytosis was observed for H1299 cells.	87
	Nile blue loaded oleyl-hyaluronan (HAC18:1) and hexyl-hyaluronan (HAC6) micelles	Clathrin, caveolae and macropinocytosis	Flow cytometric analysis revealed uptake of HAC6 micelles and HAC18:1 micelles in NHDF cells by clathrin and macropinocytosis. In HaCaT cells, uptake of HAC6 was mediated by caveolae and macropinocytic pathways while clathrin and macropinocytosis were found to be associated with the uptake of HAC18:1 micelles	166

Uptake of all the PEGylated nanoparticles proceeded *via* clathrin dependant endocytosis. Additionally, PEG1%-*g*-PLA exhibited reduced uptake following pretreatment with macropinocytic inhibitor indicating internalization *via* macropinocytosis. The difference in results could be attributed to different core/shell structure of nanoparticles resulting in altered polymer architecture. Further, the polymer architecture can be correlated to particle modulus which exhibits a low energy dependence upon fusion followed by high energy dependence during endocytosis⁹⁶. During the initial membrane bending stage the particles recognize and bind to receptors. The membrane undergoes bending and starts wrapping around particles. With increasing time, more receptors are recruited resulting in energy release which acts as driving force for wrapping. Once particles are fully wrapped, the conformational degree of freedom of the particles (polymeric chains) is reduced due to confinement within the membrane and core. Thus the surface free energy of polymer is enlarged due to steric repulsion⁹⁷. Therefore, for internalization to occur the initial binding energy must be significantly lower than energy barrier exhibited during membrane wrapping stage and subsequent endocytosis.

4.5.2. Effect of cross linking of micelles

Although extensive efforts have been made to understand the factors affecting cellular internalization of nanocarriers, there are still several parameters including the stability of nanoparticles that need an in-depth understanding and investigation. Lee et al.⁹⁸ performed comparative studies between unstable and stable nanocarriers represented by self-assembled and disulfide bonded micelles wherein, the introduction of disulfide bonds into self-assembled micelles improved the stability of micelles in physiological conditions. Self-assembled micelles (SA) were formulated from mPEG-PLA copolymer while disulfide (DS) micelles were fabricated from mPEG-(Cys)₄-PLA. To confirm the stability of DS micelles in comparison to SA micelles, cellular distribution of hydrophobic FRET probes including Dio (green) and DiI (red) in LNCap cells was visualized by FRET imaging. Following incubation for 2 h, the FRET ratio for SA micelles was found to be 0.72 and 0.32 (outside and inside the cell respectively). The fluorescence observed from SA micelles was attributed to release of fluorescent probe during micelle-membrane fusion resulting in rapid uptake *via* CME. Contrastingly, DS micelles did not exhibit fluorescence on the cell membrane following internalization indicating the maintenance of structural integrity and no decomposition upon interaction with plasma membrane. The endocytic inhibition studies were performed in LNCap cells in the presence of endocytic inhibitors. The uptake of DiI loaded SA micelles demonstrated CME while, DS micelles were internalized by both CME and macropinocytosis.

Kim et al.⁹⁹ synthesized amphiphilic block copolymer, PMMA-*b*-P(PEGMEMA) which was subsequently self-assembled into micelles. The endocytic uptake of both cross-linked micelles and non-cross linked micelles by OVCAR-3 cells was evaluated in the presence of endocytic inhibitors specific to clathrin and caveole mediated pathways. Results indicated that both micelles were internalized by caveole mediated pathway however, the uptake of cross-linked micelles was greatly inhibited in comparison non-cross-linked micelles. Greater inhibition indicates increased propensity towards internalization of *via* caveolae mediated endocytosis. Further, these cross-linked micelles also exhibited accelerated exocytosis. Sahay et al.¹⁰⁰ also fabricated polymeric micelles comprising of cross-linked ionic cores of poly(methacrylic acid) and nonionic shell of poly(ethylene oxide)

termed cl-micelles. These micelles were fluorescently labelled using FITC and subsequently internalized by MCF-7/ADR cells *via* caveole mediated endocytosis as confirmed by confocal microscopy. The micelles were also capable of bypassing early endosomes as revealed by negligible colocalization with Rab-GFP (endosomal marker).

4.5.3. Effect of polymer structure

The endocytosis of nanocarriers derived from amphiphilic copolymers is also influenced by the polymer structure including its molecular weight, ratio and nature of hydrophilic and hydrophobic segments and terminal modification. Recently Gundel et al.¹⁰¹ investigated the endocytic uptake of hydroxypropyl methacrylamide (HMPA) based polymer in different cancer cells. For this purpose, different HPMA based polymers including homopolymer, random and block copolymers with varying molecular weights (high and low) were synthesized and evaluated. The hydrophobic segment in both random and block copolymers comprised of lauryl methacrylate. The molecular weight of homopolymer varied from 12,000 to 77,000 g/mol, while random copolymers exhibited molecular weights ranging from 14,000 to 55,000 g/mol and the molecular weight of block copolymers was restricted to 12,000–21,000 g/mol. The homopolymer comprised of 100% HPMA only for both low and high molecular weight. Low molecular weight random copolymer consisted of 82% of HPMA and 18% of hydrophobic portion while high molecular weight random copolymer was more hydrophobic (25%). Finally, the low molecular weight block copolymer comprised of 21% hydrophobic segment while high molecular weight block copolymer was significantly greater in hydrophobicity (25%). The endocytosis of HPMA based copolymers was evaluated in AT1 prostate and Walker-256 mammary carcinoma cells. Endocytic uptake inhibition studies revealed that both homopolymers and block copolymers were internalized by numerous endocytic pathways (clathrin dependent, clathrin independent and macropinocytic pathways) attributed to the strong hydrophilic surface following nanoparticle formation. On the contrary, caveolae and dynamin dependant endocytosis (non-clathrin pathway) were responsible for the internalization of random copolymers (Fig. 6). This was attributed to increased lipophilicity on the outer surface in conjunction with hydrophilic groups. This could be attributed to the disordered arrangement of monomeric units in random copolymers on the surface resulting in deviation from conventional uptake mechanisms. Overall, the study indicated that a hydrophilic surface directs nanoparticle internalization by numerous endocytic pathways. While the presence of hydrophobic segments on the surface in addition to hydrophilic corona directs the particles into the cell by caveolae mediated and dynamin dependant pathways. Therefore, the endocytic uptake is affected by polymer composition including chemical structure and lipophilicity.

4.5.4. Effect of CMC

Critical micelle concentration (CMC) is a characteristic of amphiphilic block copolymers wherein, at or above CMC value, lipophilic chains form hydrophobic core of micelles surrounded by a hydrophilic shell in aqueous solution. Due to the thermodynamic nature of self-assembled micelles, a constant exchange occurs between the unimers in the micelles and those in the bulk solution resulting in the existence of both aggregation states¹⁰². Depending upon the aggregation state, amphiphilic block copolymers can undergo internalization *via* different endocytic pathways¹⁰³. Sahay et al.¹⁰⁴ investigated the endocytic uptake of

Table 6.1

Polymer structure	Monomer ratio (%)	M (g/mol)	M _w (g/mol)	D ^a	R _h (nm) ^b
Homopolymer	100	9000	12000	1.29	1.1
Homopolymer	100	52000	77000	1.49	3.0
Random copolymer	82:18	11000	14000	1.26	33.4
Random copolymer	75:25	39000	55000	1.41	35.9
Random copolymer	79:21	9000	12000	1.24	58.7
Random copolymer	75:25	17000	21000	1.24	112.8

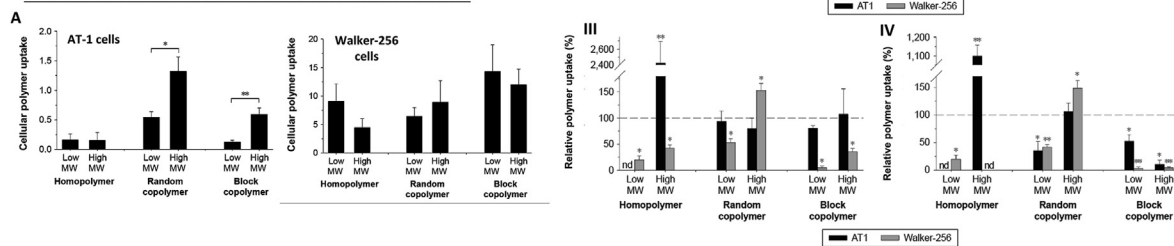


Figure 6 Effect of polymeric structure on the endocytic uptake of HMPA based polymer in different cancer cells. Table 6.1 represents the analytical data of HMPA homopolymers, random copolymer and block copolymers with low and high molecular weights. (A) Uptake studies exhibited 10-fold increase in cellular internalization in Walker-256 cells in comparison to AT-1 following incubation for 2 h. The uptake of random copolymer was greater in comparison to homopolymer and block copolymer. Block and random copolymers showed higher uptake in comparison to respective low molecular weight counterparts in AT-1. For Walker-256 cells, the uptake was independent of molecular weight and hydrodynamic radius. (B) Endocytic inhibition of polymers following pretreatment with (I) rotterlin, (II) nystatin, (III) CPZ and, (IV) dynasore in AT1 and Walker-256 cells. Both homopolymers and block copolymers were internalized by numerous endocytic pathways (clathrin dependent, clathrin independent and macropinocytosis) attributed to the strong hydrophilic surface following nanoparticle formation. On the contrary, caveolae and dynamin dependant endocytosis (non-clathrin pathway) were responsible for the internalization of random copolymers. Reprinted with permission from Ref. 101. Copyright© 2017, Dove Medical Press.

FITC labelled amphiphilic triblock copolymers of poly(ethylene oxide)-*b*-poly(propylene oxide)-*b*-poly(ethylene oxide) (PEO-PPO-PEO; Pluronic P85) in MDCK cells at different concentrations. FITC labelled P85 unimers existed at 0.001 wt% while micelles existed above the CMC value ($\sim 0.03\%$ wt) at 0.1% (*w/w*). Results indicated that P85 unimers internalized *via* caveolae mediated endocytosis while micelles internalized through clathrin mediated pathway. Further, colocalization with endocytosis markers (Cholera B toxin and transferrin) revealed that concentration of P85 above 0.01% (*w/w*), inhibited caveolae mediated endocytosis with minimal effects on clathrin mediated pathways. The probable reason for selectivity of micelles towards specific pathway may be attributed to their inhibitory ability against caveolae mediated pathway at higher concentration. Further, the outer hydrophilic portion of micelles interacted weakly with the lipid membrane in comparison to unimers containing bulky hydrophobic chains. The uptake of Pluronic carriers bearing different PEO block length and aggregation state (unimers and cross-linked micelles) has also been investigated in HeLa and U87 cancer cells. FITC labelled Pluronic, P94 and F127 unimers and micelles were selected to study their intracellular localization. The Pluronic unimers were distributed throughout the cell and nucleus which was attributed to passive diffusion while micelles remained localized. Colocalization with Lysotracker Red suggested that micelles were internalized *via* CME while unimers were internalized *via* caveolae mediated pathway into the ER and cytoplasm following which these could diffuse into the nucleus. An interesting study conducted by Miura et al.¹⁰⁵, involved the analysis of transport behavior of cationic micelles composed of a triblock copolymer of PLGA-block-branched polyethyleneimine-block-PLGA using FRET analysis. The results indicated that cationic micelles dissociated at interface between culture media and first layer of cells finally penetrating into the cells as unimers.

Pretreatment with endocytic inhibitors specific to clathrin, caveolae and macropinocytosis indicated CME and macropinocytosis as the major pathways responsible for the internalization of cationic unimers.

4.5.5. Effect of critical aggregation concentration (CAC)

Stable dispersion of hydrophobic drugs can be attained *via* fine-tuning of CAC thereby maintaining micellar integrity and avoidance of precipitation upon dilution¹⁰⁶. Various methods have been employed to determine the CAC of block copolymers including Brownian dynamics and dissipative particle dynamics (DPD) and pyrene probe method. Coarse grained molecular dynamic simulations have been carried out to elucidate the effect of aggregation number on the interaction pathways existing between plasma membrane and PCL-*b*-PEO block copolymer micelles¹⁰⁷. Four interaction pathways were discovered *viz.* attachment, semi-endocytosis, endocytosis and fusion. Endocytosis was the prominent mode of internalization of block copolymeric micelles while fusion was associated with cytotoxicity. On the basis of simulation data, it was observed that internalization pathway followed by the micelles varied with aggregation number. When the aggregation number was small (54), the micelles were semi-endocytosed by the membrane. As the aggregation number increased to 103, complete endocytosis was observed with higher bending energy ($1.1 \epsilon_0$) while excessive bending energy ($>1.3 \epsilon_0$) led to fusion pathway. Further increase in aggregation number to 141 allowed the micelles to be endocytosed with minimal bending energy ($1.0 \epsilon_0$). Thus the internalization ability of the micelles increased with higher aggregation number however, large aggregation number was associated with propensity of micelles to undergo fusion pathways leading to cytotoxicity and membrane disruption. Thus, the aggregation number needs due consideration during designing

of delivery systems as it is capable of influencing the internalization of micelles. Interestingly You et al.¹⁰⁸ investigated CAC and uptake mechanism of FITC labelled micelles prepared from stearic acid grafted chitosan oligosaccharide derivative and these were compared to self-aggregates composed of non-modified chitosan oligosaccharide in A549 cells. Results indicated that micelles were rapidly internalized with higher mean fluorescent intensities while, self-aggregates exhibited poor uptake as most of the aggregates adhered onto the cell surface and were incapable of penetrating the plasma membrane. Based on the aggregation number, it was found that self-aggregated chitosan oligosaccharides lack optimum hydrophobic domains at the surface resulting in poor cellular uptake. The aggregation number of stearic acid groups per hydrophobic microdomain was ~ 7.16 while the number of hydrophobic microdomains formed by a single chitosan-stearic acid chain was ~ 8.2 indicating that the surface of the micelles contained more hydrophobic domains resulting in development of partial hydrophobicity (minor cores) near the surface as the outer hydrophilic layer is composed of chitosan-oligosaccharide while inner core comprises of stearic acid. These minor cores can easily insert and interact with the cellular membrane thus exhibiting rapid endocytosis and endosomal escape.

4.5.6. Effect of protein corona

Upon interaction with physiological/biological fluids, nanoparticles get covered by biological macromolecules forming a protein corona. The adsorption of proteins onto the surface of nanoparticles is modulated by Columbic and van der Waal's forces, hydrophobic interactions and hydrogen bonding¹⁰⁹. Further, the amount and chemical nature of proteins adsorbed onto nanoparticles is directly correlated with the physicochemical properties of nanoparticles and the cell type¹¹⁰. The protein corona comprises of a double layer comprising of hard inner shell (irreversible binding) and dynamic outer shell which interacts weakly with the adsorbed proteins¹⁰⁹. The most common proteins involved in corona formation include opsonins (immunoglobulin, complement factor and fibrinogen) which are responsible for macrophage recognition and rapid clearance of nanoparticles from the circulation¹¹¹. Reduced efficacy, denaturation and conformational changes can be introduced in the nanocarriers following protein corona formation¹¹². Additionally, increased particle size significantly reduces cellular uptake and cell adhesion. However, reports also suggest that protein corona might be beneficial. Pre-coating of nanoparticles with human serum albumin prevents rapid clearance by RES and also modulates transient endocytic uptake switching the internalization of nanoparticles from macropinocytosis to CME leading to an altered intracellular trafficking¹¹³. Adsorption of apolipoproteins onto nanoparticles also improves transport across the blood–brain barrier (BBB)¹¹⁴. This was exemplified by transport of loperamide and dalargin across the blood brain barrier encapsulated in poly(butyl cyanoacrylate) nanoparticles coated with apolipoproteins. Results indicated significant anti-nociceptive action in comparison to uncoated nanoparticles confirming efficient transport across BBB. Moreover, the presence of preformed corona also contributed towards lowered nanoparticle aggregation and reduced toxicity. Recently Castro et al.¹¹⁵ explored the effect of plasma protein corona on the cytotoxicity and cellular uptake of sugar decorated amphiphilic nanoparticles prepared from azido-PEO-docosanoate and *N*-acetyl glucosamine (C22PEO900-GlcNAc). The uptake of uncoated and protein coated nanoparticles by Telo-RF (normal) and HeLa cells

was evaluated both qualitatively and quantitatively. The presence of protein corona reduced the uptake of coated nanoparticles in both the cells. Lowered uptake efficiency was attributed to increased size and reduced cell adhesion following protein coating. However, HeLa cells internalized greater amount of corona coated nanoparticles in comparison to Telo-RF cells. Corona coated nanoparticles also exhibited lowered cytotoxicity and hemolytic effects in normal cells and RBCs. Thus, the presence of protein corona might be beneficial if the functionality and conformation of the nanoparticles can be maintained.

4.5.7. Effect of environmental pH

The role of environmental pH is of paramount significance in cancer cells due to the existence of a pH gradient in comparison to normal cells. Although the initialization of endocytosis begins at physiological pH (7.4), subsequent pH drops to 5.5–6 within the endosomes and 5.5–5 within the lysosomes¹¹⁶. To overcome the propensity of lysosomal degradation of nanocarriers following endocytosis, pH responsive copolymers have been developed which control the cellular behaviour of nanoparticles following internalization¹¹⁷. Such nanoparticles exhibit pH-responsive properties including an efficient uptake at low and high pH values while blockage of endocytosis at neutral pH. At neutral pH, the nanoparticle protein complex (NPC) formed due to the adsorption of proteins on nanoparticles alters their biophysical properties and gets weakly associated with the membrane thereby inhibiting its endocytosis¹¹⁸. Further, it is also essential to consider the existence of pH gradient across various tumor subtypes *viz.* pH in astrocytomas is 6.5 while sacrocomas exhibit a pH value of 7. In such a case, polymers with $pK_a \sim 7.0$ could be selected enabling efficient translocation of nanoparticles into the cell interior between pH 6.5 and pH 7.5, while very few nanoparticles gain entry into the cell at pH 7.0. Additionally, polymeric nanocarriers with pK_a 7.5 can be also used to selectively target weakly acidic cells (pH 6.5) with reduced uptake at pH ~ 7.5 ^{118,119}.

5. Factors affecting intracellular fate of amphiphilic block copolymeric nanocarriers

Following cellular internalization, nanoparticles are subjected to intracellular transport and trafficking into various organelles. Similar to endocytosis, the intracellular fate of nanoparticles is dependent on the physicochemical properties including size, shape and surface chemistry along with cell type.

5.1. Trafficking into endosomes/lysosomes

Mannose-6-phosphate glycopolyptide azide end functionalized branched polycaprolactone $M^{6P}GP_{15}-(PCL_{25})_2$ was formulated into micelles with a particle size of ~ 205 nm for controlled and targeted lysosomal cargo delivery¹²⁰. Endocytic uptake studies in MDA-MB 231 cells indicated internalization of rhodamine-loaded micelles *via* CME. Further, the micelles trafficked into lysosomes upon internalization as confirmed by colocalization with Lyso-tracker green. Similarly, Li et al. investigated the intracellular fate of hydrophobically modified glycol chitosan (HGC) micelles, surface functionalized using avidin and biotin with particle size of 104.7 nm and weak cationic surface charge (+3.1 mV). The endosomal trafficking of micelles in MDA-MB 231 cells indicated that the micelles exhibited proton sponge effect resulting in

osmotic swelling and rupture of endosomal membrane followed by release into cytosol after 18 h of incubation. From the above studies it can be concluded that particles with size >80 nm are preferentially internalized *via* CME and transported to endosomes.

5.2. Trafficking into mitochondria

It has been postulated that in order to achieve complete mitochondrial localization and avoid endosomal entrapment, the particle diameter should be ~ 100 nm or less and particles should possess a positive surface charge ($>+22$ mV). Zhong et al.¹²¹ synthesized DOX derivative, conjugated acetal-PEG-PCCL (carboxylate caprolactone) micelles for the purpose of mitochondrial targeting. This was achieved by attaching lipophilic cation, (3-carboxy-propyl) triphenylphosphonium bromide (TPP) to DOX which was further conjugated to the hydrophobic end of acetal-PEG-PCCL block copolymer. The particle size was found to be ~ 100 nm and subcellular distribution of micelles was evaluated by Mitotracker Green and colocalization assay. Results indicated that micelles were capable of mitochondrial targeting as evident by the presence of yellow colour in merged images. Momekova et al.¹²² prepared mixed micellar system based on two co-assembled triblock copolymers, poly(2-(dimethylamino)ethyl methacrylate)-*b*-poly(ϵ -caprolactone)-*b*-poly(2-(dimethylamino)ethyl methacrylate) bearing TPP ligands (PDMAEMA(TPP⁺)₂₀-*b*-PCL₇₀-*b*-PDMAEMA(TPP⁺)₂₀) and poly(ethylene oxide)-*b*-poly(ϵ -caprolactone)-*b*-poly(ethylene oxide) (PEO₁₁₃-*b*-PCL₇₀-*b*-PEO₁₁₃) for mitochondrial delivery of curcumin. The hydrodynamic diameter of these micelles was ~ 52 nm and exhibited a positive surface potential ($+27.5$ mV). Colocalization with Mitotracker indicated successful intracellular accumulation of these nanocarriers into the mitochondria of PC-3 cells. Similarly Chen et al.¹²³, formulated hybrid micelles of Soluplus (polyvinyl caprolactam-polyvinyl acetate-polyethylene glycol)/*D*- α -tocopherol acid polyethylene glycol 1000 succinate (TPGS)/dequalinium (DQA) for mitochondrial targeting. The particle size of micelles was ~ 65 nm and possessed weak cationic surface charge ($+2.34$ mV). The micelles induced mitochondria mediated apoptosis as evident by the generation of high ROS and decreased mitochondrial depolarization indicating that the micelles were specifically delivered into the mitochondria.

5.3. Trafficking into perinuclear region and Golgi

Intracellular trafficking of nanocarriers into the perinuclear region and Golgi usually involves internalization *via* caveolae mediated pathways. Debnath et al.¹²⁴ designed polymeric micelles based on polyaspartic acid backbone with hydrophobic oleyl groups with an average particle size of ~ 30 nm with negative zeta-potential (-10 mV). Experimental studies revealed that micelles internalized into HT22 neuronal cells *via* caveolae mediated pathway and trafficked into the perinuclear region within 6 h with minimal lysosomal entrapment. Similarly Qu et al.¹²⁵ investigated the intracellular trafficking of micelles fabricated using poly(2-ethyl-2-oxazoline)-vitamin E succinate (PEOz-VES) and TPGS1000. The particle size of micelles was ~ 20 nm, possessed a weak cationic charge ($\sim +2$ mV) and internalized into Caco-2 cells *via* clathrin and caveolae mediated pathways. Thus, micelles

exhibited intracellular accumulation into endosomes, Golgi and mitochondria following internalization which was confirmed by confocal microscopy using suitable markers. Particles possessing weak anionic surface charge (~ -5 to -10 mV) and lipophilic groups predominantly interact with membrane (sphingolipids) on account of their hydrophobicity. Further, particle size <80 nm is preferred for uptake *via* caveolae mediated endocytosis. Additionally, trafficking into lysosomes and Golgi can be achieved *via* surface modification of cationic nanocarriers (<10 mV) with anionic molecules while undergoing internalization *via* both clathrin and caveolae mediated pathways.

6. Conclusions and future perspectives

Inspite of the experimental findings and availability of several reviews, it is difficult to propose general guidelines regarding the designing of an ideal amphiphilic polymer based nanocarrier to be internalized *via* specific endocytic mechanism as the rate and mechanism of endocytosis is found to be dependant on several factors as discussed in the previous sections. However, once inside the cells, caveolae mediated pathway is highly suitable for the delivery of nanoparticles due to its ability to bypass the lysosomal compartment and avoid degradation. Further, caveolae mediated endocytosis trafficks the particles *via* caveosomes having neutral pH with minimal chances of degradation. Thus, for nanoparticles, it is preferred to bypass the lysosomes and avoid enzymatic degradation and hence caveolae mediated pathway is preferred over CME¹²⁶.

Particle size: Based on the reported literature, we believe that particles with size ranging between 10 and ~ 100 nm are ideal for cellular internalization due to their rapid uptake *via* clathrin and caveolae mediated pathways¹²⁷. Increased particle size (>200 nm) not only presents physical difficulties for the nanoparticles during translocation across the lipid bilayer but are also susceptible to undergo engulfment *via* macropinocytosis¹²⁸. Moreover, theoretical calculations have also revealed that nanoparticles with a radius of 27–30 nm exhibit rapid endocytosis with least internalization time. However, such specificity presents a challenge as most nanoparticles enter through and fail to localize into the target subcellular compartments including nucleus, mitochondria and golgi apparatus. Further, nanoparticle agglomeration under physiological conditions should also be studied by morphological and physical characterization using multiple characterization techniques like SEM, TEM, AFM in aqueous and biological media to ensure the accuracy of experimental data.

Surface charge and hydro/lipo-philicity: The surface charge plays an important role in controlling the initial interaction between lipid membrane and nanoparticles. Secondly, the hydrophobicity/lipophilicity along with size is another factor controlling the interaction of nanoparticles with cell membrane. It has been observed that lipophilic anionic nanoparticles interact with cell membrane by hydrophobic interactions and either remain bound to the membrane or internalize *via* CME¹²⁹. Similarly, lipophilic cationic particles would seemingly exhibit stronger interaction and higher cytotoxicity. To overcome this, lipophilic zwitterionic nanoparticles can be formulated with low anionic surface charge. These particles would interact weakly with the cells and internalize *via* caveolae mediated pathways

and pose insignificant cytotoxicity⁴. Finally, cationic nanoparticles favour CME *via* electrostatic interaction with receptor proteins specific to clathrin while particles with low surface charge and lipophilic groups interact with lipidic rafts *via* hydrophobic interactions due to the presence of lipophilic chemical groups triggering caveolae mediated endocytosis.

Shape: Both shape anisotropy and initial orientation of nanoparticles are crucial for determining the interaction and uptake kinetics of the particles with respect to lipidic bilayer¹³⁰. Interestingly, nanoparticles of varying shapes (rod, ellipsoidal, cylindrical, and cubical) can rotate themselves onto sharp edges to enhance their penetration capability. This in turn is controlled by contact area between the particle and membrane and curvature of the particle at the point of contact. It is widely believed that membrane proteins insert protein segments into the lipid bilayer of the membrane and thus induce intracellular membrane curvature/bending or these can also induce shape effect following adhesion of curved protein domain to membrane domain¹³¹. One of the most common modes of membrane bending occurs *via* the assembly of clathrin protein scaffold and protein–protein interaction with BAR protein (Bin/amphiphysin/Rvs), EHD (Eps15 homology) domain proteins, synaptogamin and dynamin¹³². Using Martini coarse grained simulation studies, it was inferred that translocation time for spherical nanoparticles was the least in comparison cubical and rod shaped nanoparticles. Similarly, it is difficult to endocytose ellipsoidal particles in comparison to spherical nanoparticles on account of their higher curvature thus requiring higher membrane bending energy¹³³. However, sphere may not be the optimal shape for internalization as prolate shape of spherocylinders can lead to a more efficient delivery in comparison to spherical particles of same diameter due to larger volume possessed by the spherocylindrical particles resulting in faster uptake kinetics¹³⁴.

In order to develop particles which are monodisperse in nature; a top down fabrication technique termed as particle replication in non-wetting templates (PRINT) can be employed which is capable of producing particles with uniform size, shape and surface chemistry. PRINT is a continuous high resolution molding technology which enables precise designing and synthesis of micro and nanoparticles. This GMP compliant technology couples soft lithographic techniques with roll-to-roll processes to serve as a platform for particle fabrication at a large scale and with complete control over their physicochemical properties¹³⁵. Endocytic inhibition studies revealed that caveolae mediated endocytosis was evident for the uptake for both asymmetrical PRINT cylindrical nanoparticles with high aspect ratio (AR = 3) and symmetrical PRINT cylindrical nanoparticles (AR = 1). Another factor associated with particle shape during endocytosis is nanoparticle stiffness. It has been elucidated that in comparison to soft nanoparticles, rigid nanoparticles underwent complete membrane wrapping; this is attributed to the large bending energy barrier needed to be overcome by the cell membrane to uptake soft nanoparticles on account of larger curvature due to particle deformation. Thus nanoparticulate drug delivery can be further advanced by considering the shape of particles¹³⁶.

Cell type: The most challenging and poorly explored area in relation to nanoparticle endocytosis is the selection of cell type in elucidating the entry and fate of nanoparticles within the cells. As most cell lines are derived from various sources, current studies fail to establish a correlation between the origin of a cell and endocytic pathways that a nanocarrier would follow¹³⁷. Thus it is

recommended to carry out the endocytic investigations of nanoparticles in multiple cell types to rule out cellular heterogeneity and phenotypic variation since the amount of protein associated with clathrin and caveolae mediated endocytosis varies from cell to cell. For verifying the participation of caveolae mediated internalization, uptake studies can be performed in endothelial cells, fibroblastic cells and Caco-2 cells which are abundant in Cav-1 protein while other cells including neurons and leukocytes cannot utilize this pathway as they lack Cav-1 protein.

Another caveat in the endocytic uptake studies are the conditions maintained during the *in-vitro* cell culture experiments. Reports indicate that selection of culture medium affects the endocytosis of nanoparticles. Further, the effect of cell density and presence/absence of growth factors including platelet-derived growth factor (PDGF), epidermal growth factor (EGF), fibroblast growth factor (FGF) also influence cellular uptake of nanocarriers. Haniu et al.¹³⁸ investigated the effect of culture medium on the endocytosis of multi-walled carbon nanotubes (MWCNT) in BEAS-2B cells. For this purpose, the uptake was evaluated in cells supplemented with two types of culture media (Ham's F12 containing 10% FBS and serum-free growth medium [SFGM]). Results revealed that MWCNT underwent internalization into BEAS-2B cells cultured only in Ham's F12 media but not in SFGM. Thus, experimental design involving endocytosis should focus on including multiple cell types under different growth conditions to gain better understanding.

Understanding the cellular internalization of nanoparticulate systems has become central to the field of drug delivery. Nanoparticles utilize various endocytic vesicles followed by complex trafficking mechanisms to sort towards specific intracellular organelles. Based on the reported examples, it can be concluded that particle size, shape, surface charge and chemistry are critical physicochemical parameters modulating the entry of nanocarriers through defined endocytic routes. However, there is continuous need for the development of novel tools which can provide an in depth understanding of cellular interaction with nanocarriers depending on cell phenotype, growth conditions and cell density. Thus, development of robust assays to elucidate endocytic mechanisms under *in-vivo* conditions needs consideration. Development of such *in vivo* assays to study endocytosis of nanomedicines is further complicated by extensive opsonization and remodelling that nanocarriers undergo under physiological conditions. Safety consideration of nanocarriers including immunogenicity and cytotoxicity which can disrupt or modify endocytic machinery should also be carefully investigated. Certain reports also suggest that targeted nanocarriers with biospecific ligand might possess different endocytic route in comparison to nanocarrier without ligand. Therefore selection of targeting ligand should also be taken into account for designing of a nanocarrier towards a specific endocytic pathway. From a clinical viewpoint, patient samples can be screened to check alteration in proteins involved in endocytic machinery which can further be correlated to improve the clinical performance of nanocarriers. Additionally, identification of trafficking biomarkers in patient samples could significantly benefit therapeutic outcomes and accelerate clinical development of nanomedicines.

Disease related modification and treatment induced alteration in endolysosomal system disrupts membrane trafficking pathways along with mutations in accessory or cargo proteins. Breast cancer induces mutations in Cav-1 protein and loss/lack of Cav-1 leads to progression of the cancer. Similarly, mutations are also observed

in autosomal recessive hypercholesterolemia (ARH) wherein, LDL receptor adaptor proteins and ARH protein linked to CCP are transformed. Auto-immune diseases are correlated with desmosomal cadherin Dsg3 which is a cell adhesion molecule and is endocytosed *via* clathrin and dynamin independent pathways in the presence of antibodies and are degraded resulting in loss of cell adhesion. Pemphigus vulgaris is an autoimmune disease which is characterized by mucosal erosion and blistering. Autoantibodies are generated against desmosomal cadherin Dsg3 which is a cell adhesion molecule and complexes are formed. These complexes undergo internalization *via* clathrin and dynamin independent pathways and degraded¹³⁹. Based on the examples reported, it can be concluded that in lieu of critical physicochemical parameters affecting internalization and intracellular fate of amphiphilic nanocarriers additional investigation of miscellaneous properties would facilitate the designing and development of nanocarriers specific to particular endocytic route.

Acknowledgments

This work was financially sponsored by extramural research funding support from Department of Science and Technology, Rajasthan (Project #P.7 (3) Wipro/R&D/2016/6009, India). The authors have no other relevant affiliation or financial support with any organization with a financial interest in or financial conflict with the subject matter or materials discussed in the manuscript apart from those disclosed. We also acknowledge Biorender for their technical support in the creation of the figures.

Author contributions

Anupama Mittal and Deepak Chitkara designed the theme and concept of the manuscript. Samrat Mazumdar was responsible for acquisition, analysis, interpretation and compilation of the articles. Samrat Mazumdar, Deepak Chitkara and Anupama Mittal drafted and critically reviewed the manuscript.

Conflicts of interest

The authors (Deepak Chitkara and Anupama Mittal) are the founding directors of Nanobrid Innovations Private Limited that is involved in the development of nanotechnology based products. They have business and/or financial interest in the operations of the company. The same could be disclosed on request. The authors declare that they have no conflict of interest pertaining to the work outlined in this study.

References

1. Patra JK, Das G, Fraceto LF, Campos EVR, del Pilar Rodriguez-Torres M, Acosta-Torres LS, et al. Nano based drug delivery systems: recent developments and future prospects. *J Nanobiotechnol* 2018; **16**:71.
2. Caster JM, Patel AN, Zhang T, Wang A. Investigational nanomedicines in 2016: a review of nanotherapeutics currently undergoing clinical trials. *Wiley Interdiscip Rev Nanomed* 2017; **9**:e1416.
3. Meng H, Leong W, Leong KW, Chen C, Zhao Y. Walking the line: the fate of nanomaterials at biological barriers. *Biomaterials* 2018; **174**:41–53.
4. Chakraborty A, Jana NR. Clathrin to lipid raft-endocytosis *via* controlled surface chemistry and efficient perinuclear targeting of nanoparticle. *J Phys Chem Lett* 2015; **6**:3688–97.
5. Donahue ND, Acar H, Wilhelm S. Concepts of nanoparticle cellular uptake, intracellular trafficking, and kinetics in nanomedicine. *Adv Drug Deliv Rev* 2019; **143**:68–96.
6. Agudo-Canalejo J, Lipowsky R. Critical particle sizes for the engulfment of nanoparticles by membranes and vesicles with bilayer asymmetry. *ACS Nano* 2015; **9**:3704–20.
7. Wu LG, Hamid E, Shin W, Chiang HC. Exocytosis and endocytosis: modes, functions, and coupling mechanisms. *Annu Rev Physiol* 2014; **76**:301–31.
8. Zhang B, Koh YH, Beckstead RB, Budnik V, Ganetzky B, Bellen HJ. Synaptic vesicle size and number are regulated by a clathrin adaptor protein required for endocytosis. *Neuron* 1998; **21**:1465–75.
9. Miller SE, Sahlender DA, Graham SC, Höning S, Robinson MS, Peden AA, et al. The molecular basis for the endocytosis of small R-SNAREs by the clathrin adaptor CALM. *Cell* 2011; **147**:1118–31.
10. Cremaschi D, Porta C, Ghirardelli R, Manzoni C, Caremi I. Endocytosis inhibitors abolish the active transport of polypeptides in the mucosa of the nasal upper concha of the rabbit. *Biochim Biophys Acta Biomembr* 1996; **1280**:27–33.
11. Yang NJ, Hinner MJ. Getting across the cell membrane: an overview for small molecules, peptides, and proteins. In: Gautier A, Hinner M, editors. *Site-specific protein labeling. Methods in molecular biology*, vol. 1266. New York: Humana Press; 2015. p. 29–53.
12. Behzadi S, Serpooshan V, Tao W, Hamaly MA, Alkawareek MY, Dreden EC, et al. Cellular uptake of nanoparticles: journey inside the cell. *Chem Soc Rev* 2017; **46**:4218–44.
13. Prietl B, Meindl C, Roblegg E, Pieber T, Lanzer G, Fröhlich E. Nano-sized and micro-sized polystyrene particles affect phagocyte function. *Cell Biol Toxicol* 2014; **30**:1–16.
14. Gustafson HH, Holt-Casper D, Grainger DW, Ghandehari H. Nanoparticle uptake: the phagocyte problem. *Nano Today* 2015; **10**:487–510.
15. Polando RE, Jones BC, Ricardo C, Whitcomb J, Ballhorn W, McDowell MA. Mannose receptor (MR) and Toll-like receptor 2 (TLR2) influence phagosome maturation during Leishmania infection. *Parasite Immunol* 2018; **40**:e12521.
16. Levin R, Grinstein S, Canton J. The life cycle of phagosomes: formation, maturation, and resolution. *Immunol Rev* 2016; **273**:156–79.
17. Kaksonen M, Roux A. Mechanisms of clathrin-mediated endocytosis. *Nat Rev Mol Cell* 2018; **19**:313.
18. Sochacki KA, Dickey AM, Strub M-P, Taraska JW. Endocytic proteins are partitioned at the edge of the clathrin lattice in mammalian cells. *Nat Cell Biol* 2017; **19**:352–61.
19. Li R, Xie Y. Nanodrug delivery systems for targeting the endogenous tumor microenvironment and simultaneously overcoming multidrug resistance properties. *J Control Release* 2017; **251**:49–67.
20. Puangmalai N, Bhatt N, Montalbano M, Sengupta U, Gaikwad S, Ventura F, et al. Internalization mechanisms of brain-derived tau oligomers from patients with Alzheimer's disease, progressive supranuclear palsy and dementia with Lewy bodies. *Cell Death Dis* 2020; **11**:1–16.
21. Vykoukal J, Fahrman J, Thompson T. Caveolin and lipid domains—close companions in managing cellular pathways. *Cancer Metastasis Rev* 2020; **39**:341–2.
22. Parton RG, McMahon KA, Wu Y. Caveolae: formation, dynamics, and function. *Curr Opin Cell Biol* 2020; **65**:8–16.
23. Dudău M, Codrici E, Tanase C, Gherghiceanu M, Enciu AM, Hinescu ME. Caveolae as potential hijackable gates in cell communication. *Front Cell Dev Biol* 2020; **8**:581732.
24. Miele E, Spinelli GP, Miele E, Tomao F, Tomao S. Albumin-bound formulation of paclitaxel (Abraxane® ABI-007) in the treatment of breast cancer. *Int J Nanomed* 2009; **4**:99.
25. Liu CG, Han YH, Kankala RK, Wang SB, Chen AZ. Subcellular performance of nanoparticles in cancer therapy. *Int J Nanomed* 2020; **15**:675.
26. Recouvreux MV, Commisso C. Macropinocytosis: a metabolic adaptation to nutrient stress in cancer. *Front Endocrinol* 2017; **8**:261.
27. Stow JL, Hung Y, Wall AA. Macropinocytosis: insights from immunology and cancer. *Curr Opin Cell Biol* 2020; **65**:131–40.

28. Falcone S, Cocucci E, Podini P, Kirchhausen T, Clementi E, Meldolesi J. Macropinocytosis: regulated coordination of endocytic and exocytic membrane traffic events. *J Cell Sci* 2006;**119**: 4758–69.
29. Ha KD, Bidlingmaier SM, Liu B. Macropinocytosis exploitation by cancers and cancer therapeutics. *Front Physiol* 2016;**7**:381.
30. Huang JL, Jiang G, Song QX, Gu X, Hu M, Wang XL, et al. Lipoprotein-biomimetic nanostructure enables efficient targeting delivery of siRNA to Ras-activated glioblastoma cells via macropinocytosis. *Nat Commun* 2017;**8**:1–18.
31. Liu Z, Roche PA. Macropinocytosis in phagocytes: regulation of MHC class-II-restricted antigen presentation in dendritic cells. *Front Physiol* 2015;**6**:1.
32. Gratton SE, Ropp PA, Pohlhaus PD, Luft JC, Madden VJ, Napier ME, et al. The effect of particle design on cellular internalization pathways. *Proc Natl Acad Sci U S A* 2008;**105**:11613–8.
33. Zhang H, Ji Q, Huang C, Zhang S, Yuan B, Yang K, et al. Cooperative transmembrane penetration of nanoparticles. *Sci Rep* 2015;**5**: 10525.
34. Shil P, Achary KB, Alagarasu K. Numerical analyses of electroporation-mediated doxorubicin uptake in eukaryotic cells: role of membrane cholesterol content. *Indian J Biochem Biophys* 2018;**55**:52–61.
35. Remaut K, Oorschot V, Braeckmans K, Klumperman J, De Smedt SC. Lysosomal capturing of cytoplasmic injected nanoparticles by autophagy: an additional barrier to non viral gene delivery. *J Control Release* 2014;**195**:29–36.
36. Letchford K, Burt H. A review of the formation and classification of amphiphilic block copolymer nanoparticulate structures: micelles, nanospheres, nanocapsules and polymersomes. *Eur J Pharm Biopharm* 2007;**65**:259–69.
37. Alexandridis P. Amphiphilic copolymers and their applications. *Curr Opin Colloid Interface Sci* 1996;**1**:490–501.
38. Hanafy NA, El-Kemary M, Leporatti S. Micelles structure development as a strategy to improve smart cancer therapy. *Cancers* 2018;**10**:238.
39. Sant S, Poulin S, Hildgen P. Effect of polymer architecture on surface properties, plasma protein adsorption, and cellular interactions of pegylated nanoparticles. *J Biomed Mater Res* 2008;**87**:885–95.
40. Chen J, Lin Y, Chen Y, Koning CE, Wu J, Wang H. Low-crystallinity to highly amorphous copolyesters with high glass transition temperatures based on rigid carbohydrate-derived building blocks. *Polym Int* 2021;**70**:536–45.
41. Martin C, Aibani N, Callan JF, Callan B. Recent advances in amphiphilic polymers for simultaneous delivery of hydrophobic and hydrophilic drugs. *Ther Deliv* 2016;**7**:15–31.
42. Xu Q, Li S, Yu C, Zhou Y. Self-assembly of amphiphilic alternating copolymers. *Chem Eur J* 2019;**25**:4255–64.
43. Varlas S, Lawrenson SB, Arkinstall LA, O'Reilly RK, Foster JC. Self-assembled nanostructures from amphiphilic block copolymers prepared via ring-opening metathesis polymerization (ROMP). *Prog Polym Sci* 2020;**107**:101278.
44. Henriksen-Lacey M, Carregal-Romero S, Liz-Marzán LM. Current challenges toward *in vitro* cellular validation of inorganic nanoparticles. *Bioconjugate Chem* 2017;**28**:212–21.
45. Roursgaard M, Knudsen KB, Northeved H, Persson M, Christensen T, Kumar PE, et al. *In vitro* toxicity of cationic micelles and liposomes in cultured human hepatocyte (HepG2) and lung epithelial (A549) cell lines. *Toxicol Vitro* 2016;**36**:164–71.
46. Knudsen KB, Northeved H, Ek PK, Permin A, Gjetting T, Andresen TL, et al. *In vivo* toxicity of cationic micelles and liposomes. *Nanomedicine* 2015;**11**:467–77.
47. Leupold E, Nikolenko H, Beyermann M, Dathe M. Insight into the role of HSPG in the cellular uptake of apolipoprotein E-derived peptide micelles and liposomes. *Biochim Biophys Acta Biomembr* 2008;**1778**:2781–9.
48. Iversen T-G, Skotland T, Sandvig K. Endocytosis and intracellular transport of nanoparticles: present knowledge and need for future studies. *Nano Today* 2011;**6**:176–85.
49. Sahay G, Alakhova DY, Kabanov AV. Endocytosis of nanomedicines. *J Control Release* 2010;**145**:182–95.
50. Duan X, Li Y. Physicochemical characteristics of nanoparticles affect circulation, biodistribution, cellular internalization, and trafficking. *Small* 2013;**9**:1521–32.
51. Jiang L, Li X, Liu L, Zhang Q. Cellular uptake mechanism and intracellular fate of hydrophobically modified pullulan nanoparticles. *Int J Nanomed* 2013;**8**:1825.
52. Liu P, Sun Y, Wang Q, Sun Y, Li H, Duan Y. Intracellular trafficking and cellular uptake mechanism of mPEG-PLGA-PLL and mPEG-PLGA-PLL-Gal nanoparticles for targeted delivery to hepatomas. *Biomaterials* 2014;**35**:760–70.
53. Xin H, Jiang X, Gu J, Sha X, Chen L, Law K, et al. Angiopoep-conjugated poly (ethylene glycol)-*co*-poly(ϵ -caprolactone) nanoparticles as dual-targeting drug delivery system for brain glioma. *Biomaterials* 2011;**32**:4293–305.
54. Nam HY, Kwon SM, Chung H, Lee SY, Kwon SH, Jeon H, et al. Cellular uptake mechanism and intracellular fate of hydrophobically modified glycol chitosan nanoparticles. *J Control Release* 2009;**135**: 259–67.
55. Suen WLL, Chau Y. Size-dependent internalisation of folate-decorated nanoparticles via the pathways of clathrin and caveolae-mediated endocytosis in ARPE-19 cells. *J Pharm Pharmacol* 2014;**66**:564–73.
56. Zhao J, Stenzel MH. Entry of nanoparticles into cells: the importance of nanoparticle properties. *Polym Chem* 2018;**9**:259–72.
57. Hassan SA. Computational study of the forces driving aggregation of ultrasmall nanoparticles in biological fluids. *ACS Nano* 2017;**11**: 4145–54.
58. Bhattacharjee S, Ershov D, Fytianos K, van der Gucht J, Alink GM, Rietjens IM, et al. Cytotoxicity and cellular uptake of tri-block copolymer nanoparticles with different size and surface characteristics. *Part Fibre Toxicol* 2012;**9**:1–19.
59. Niu Y, Zhang B, Galluzzi M. An amphiphilic aggregate-induced emission polyurethane probe for *in situ* actin observation in living cells. *J Colloid Interface Sci* 2020;**582**:1191–202.
60. Verma A, Uzun O, Hu Y, Han H-S, Watson N, et al. Surface-structure-regulated cell-membrane penetration by monolayer-protected nanoparticles. *Nat Mater* 2008;**7**:588–95.
61. Van Lehn RC, Alexander-Katz A. Energy landscape for the insertion of amphiphilic nanoparticles into lipid membranes: a computational study. *PLoS One* 2019;**14**:e0209492.
62. Van Lehn RC, Alexander-Katz A. Pathway for insertion of amphiphilic nanoparticles into defect-free lipid bilayers from atomistic molecular dynamics simulations. *Soft Matter* 2015;**11**:3165–75.
63. Wang Z, Wu Z, Liu J, Zhang W. Particle morphology: an important factor affecting drug delivery by nanocarriers into solid tumors. *Expert Opin Drug Deliv* 2018;**15**:379–95.
64. Huang C, Zhang Y, Yuan H, Gao H, Zhang S. Role of nanoparticle geometry in endocytosis: laying down to stand up. *Nano Lett* 2013;**13**:4546–50.
65. Krauss M, Haucke V. Shaping membranes for endocytosis. In: Amara SG, Bamberg E, Fleischmann BK, Gudermann T, Jahn R, Lederer WJ, et al., editors. *Reviews of physiology, biochemistry and pharmacology*, vol. 161. Berlin: Springer; 2009. p. 45–66.
66. Li D, Tang Z, Gao Y, Sun H, Zhou S. A bio-inspired rod-shaped nanoplatform for strongly infecting tumor cells and enhancing the delivery efficiency of anticancer drugs. *Adv Funct Mater* 2016;**26**: 66–79.
67. Hu X, Hu J, Tian J, Ge Z, Zhang G, Luo K, et al. Polyprodrug amphiphiles: hierarchical assemblies for shape-regulated cellular internalization, trafficking, and drug delivery. *J Am Chem Soc* 2013;**135**:17617–29.

68. Deng H, Dutta P, Liu J. Entry modes of ellipsoidal nanoparticles on a membrane during clathrin-mediated endocytosis. *Soft Matter* 2019; **15**:5128–37.
69. Geng Y, Dalhaimer P, Cai S, Tsai R, Tewari M, Minko T, et al. Shape effects of filaments versus spherical particles in flow and drug delivery. *Nat Nanotechnol* 2007; **2**:249–55.
70. Raman AS, Pajak J, Chiew Y. Interaction of PCL based self-assembled nano-polymeric micelles with model lipid bilayers using coarse-grained molecular dynamics simulations. *Chem Phys Lett* 2018; **712**:1–6.
71. Van Lehn RC, Atukorale PU, Carney RP, Yang YS, Stellacci F, Irvine DJ, et al. Effect of particle diameter and surface composition on the spontaneous fusion of monolayer-protected gold nanoparticles with lipid bilayers. *Nano Lett* 2013; **13**:4060–7.
72. Gkeka P, Angelikopoulos P, Sarkisov L, Cournia Z. Membrane partitioning of anionic, ligand-coated nanoparticles is accompanied by ligand snorkeling, local disordering, and cholesterol depletion. *PLoS Comput Biol* 2014; **10**:e1003917.
73. Zhang Z, Lin X, Gu N. Effects of temperature and PEG grafting density on the translocation of PEGylated nanoparticles across asymmetric lipid membrane. *Colloids Surf, B* 2017; **160**:92–100.
74. Wiemann JT, Shen Z, Ye H, Li Y, Yu Y. Membrane poration, wrinkling, and compression: deformations of lipid vesicles induced by amphiphilic Janus nanoparticles. *Nanoscale* 2020; **12**:20326–36.
75. Wang W, Zhang J, Li C, Huang P, Gao S, Han S, et al. Facile access to cytocompatible multicompartiment micelles with adjustable Janus-cores from A-block-b-graft-C terpolymers prepared by combination of ROP and ATRP. *Colloids Surf, B* 2014; **115**:302–9.
76. Brendel JC, Sanchis J, Catrouillet S, Czuba E, Chen MZ, Long BM, et al. Secondary self-assembly of supramolecular nanotubes into tubisomes and their activity on cells. *Angew Chem Int* 2018; **57**:16678–82.
77. Cui F, Lin J, Li Y, Li Y, Wu H, Yu F, et al. Bacillus-shape design of polymer based drug delivery systems with Janus-faced function for synergistic targeted drug delivery and more effective cancer therapy. *Mol Pharm* 2015; **12**:1318–27.
78. Linares J, Matesanz MCn, Vila M, Feito MJ, Goncalves G, Vallet-Regí M, et al. Endocytic mechanisms of graphene oxide nanosheets in osteoblasts, hepatocytes and macrophages. *ACS Appl Mater Interfaces* 2014; **6**:13697–706.
79. Mao J, Chen P, Liang J, Guo R, Yan LT. Receptor-mediated endocytosis of two-dimensional nanomaterials undergoes flat vesiculation and occurs by revolution and self-rotation. *ACS Nano* 2016; **10**:1493–502.
80. Suk JS, Xu Q, Kim N, Hanes J, Ensign LM. PEGylation as a strategy for improving nanoparticle-based drug and gene delivery. *Adv Drug Deliv Rev* 2016; **99**:28–51.
81. Yameen B, Choi WI, Vilos C, Swami A, Shi J, Farokhzad OC. Insight into nanoparticle cellular uptake and intracellular targeting. *J Control Release* 2014; **190**:485–99.
82. Harush-Frenkel O, Rozentur E, Benita S, Altschuler Y. Surface charge of nanoparticles determines their endocytic and transcytotic pathway in polarized MDCK cells. *Biomacromolecules* 2008; **9**:435–43.
83. Pang Z, Gao H, Chen J, Shen S, Zhang B, Ren J, et al. Intracellular delivery mechanism and brain delivery kinetics of biodegradable cationic bovine serum albumin-conjugated polymersomes. *Int J Nanomed* 2012; **7**:3421.
84. Xiao K, Li Y, Luo J, Lee JS, Xiao W, Gonik AM, et al. The effect of surface charge on *in vivo* biodistribution of PEG-oligocholeic acid based micellar nanoparticles. *Biomaterials* 2011; **32**:3435–46.
85. Bhattacharjee S, Ershov D, vdGucht J, Alink GM, Rietjens IMM, Zuilhof H, et al. Surface charge-specific cytotoxicity and cellular uptake of tri-block copolymer nanoparticles. *Nanotoxicology* 2013; **7**:71–84.
86. Fernandez-Rojo MA, Ramm GA. Caveolin-1 function in liver physiology and disease. *Trends Mol Med* 2016; **22**:889–904.
87. Liu YS, Cheng RY, Lo YL, Hsu C, Chen SH, Chiu CC, et al. Distinct CPT-induced deaths in lung cancer cells caused by clathrin-mediated internalization of CP micelles. *Nanoscale* 2016; **8**:3510–22.
88. Zhou Z, Li L, Yang Y, Xu X, Huang Y. Tumor targeting by pH-sensitive, biodegradable, cross-linked N-(2-hydroxypropyl) methacrylamide copolymer micelles. *Biomaterials* 2014; **35**:6622–35.
89. Qiu L, Shan X, Long M, Ahmed KS, Zhao L, Mao J, et al. Elucidation of cellular uptake and intracellular trafficking of heparosan polysaccharide-based micelles in various cancer cells. *Int J Biol Macromol* 2019; **130**:755–64.
90. Hu X, Yang FF, Liu CY, Ehrhardt C, Liao YH. *In vitro* uptake and transport studies of PEG-PLGA polymeric micelles in respiratory epithelial cells. *Eur J Pharm Biopharm* 2017; **114**:29–37.
91. Serpooshan V, Sheibani S, Pushparaj P, Wojcik M, Jang AY, Santos MR, et al. Effect of cell sex on uptake of nanoparticles: the overlooked factor at the nanobio interface. *ACS Nano* 2018; **12**:2253–66.
92. Foroozandeh P, Aziz AA, Mahmoudi M. Effect of cell age on uptake and toxicity of nanoparticles: the overlooked factor at the nanobio interface. *ACS Appl Mater Interfaces* 2019; **11**:39672–87.
93. Farvadi F, Ghahremani MH, Hashemi F, Hormozi-Nezhad MR, Raoufi M, Zanganeh S, et al. Cell shape affects nanoparticle uptake and toxicity: an overlooked factor at the nanobio interfaces. *J Colloid Interface Sci* 2018; **531**:245–52.
94. Yang C, Gao S, Dagnæs-Hansen F, Jakobsen M, Kjems J. Impact of PEG chain length on the physical properties and bioactivity of PEGylated chitosan/siRNA nanoparticles *in vitro* and *in vivo*. *ACS Appl Mater Interfaces* 2017; **9**:12203–16.
95. Ibricevic A, Guntsen SP, Zhang K, Shrestha R, Liu Y, Sun JY, et al. PEGylation of cationic, shell-crosslinked-knedel-like nanoparticles modulates inflammation and enhances cellular uptake in the lung. *Nanomedicine* 2013; **9**:912–22.
96. Guo P, Liu D, Subramanyam K, Wang B, Yang J, Huang J, et al. Nanoparticle elasticity directs tumor uptake. *Nat Commun* 2018; **9**:1–9.
97. Li Y, Kröger M, Liu WK. Endocytosis of PEGylated nanoparticles accompanied by structural and free energy changes of the grafted polyethylene glycol. *Biomaterials* 2014; **35**:8467–78.
98. Lee SY, Tyler JY, Kim S, Park K, Cheng JX. FRET imaging reveals different cellular entry routes of self-assembled and disulfide bonded polymeric micelles. *Mol Pharm* 2013; **10**:3497–506.
99. Kim Y, Pourgholami MH, Morris DL, Lu H, Stenzel MH. Effect of shell-crosslinking of micelles on endocytosis and exocytosis: acceleration of exocytosis by crosslinking. *Biomater Sci* 2013; **1**:265–75.
100. Sahay G, Kim JO, Kabanov AV, Bronich TK. The exploitation of differential endocytic pathways in normal and tumor cells in the selective targeting of nanoparticulate chemotherapeutic agents. *Biomaterials* 2010; **31**:923–33.
101. Gündel D, Allmeroth M, Reime S, Zentel R, Thews O. Endocytotic uptake of HPMA-based polymers by different cancer cells: impact of extracellular acidosis and hypoxia. *Int J Nanomed* 2017; **12**:5571.
102. Deshmukh AS, Chauhan PN, Noolvi MN, Chaturvedi K, Ganguly K, Shukla SS, et al. Polymeric micelles: basic research to clinical practice. *Int J Pharm* 2017; **532**:249–68.
103. Sahay G, Batrakova EV, Kabanov AV. Different internalization pathways of polymeric micelles and unimers and their effects on vesicular transport. *Bioconjugate Chem* 2008; **19**:2023–9.
104. Arranja A, Denkova AG, Morawska K, Waton G, Van Vlierberghe S, Dubruel P, et al. Interactions of Pluronic nanocarriers with 2D and 3D cell cultures: effects of PEO block length and aggregation state. *J Control Release* 2016; **224**:126–35.
105. Miura S, Suzuki H, Bae YH. A multilayered cell culture model for transport study in solid tumors: evaluation of tissue penetration of polyethyleneimine based cationic micelles. *Nano Today* 2014; **9**:695–704.
106. Aydin F, Chu X, Uppaladadiam G, Devore D, Goyal R, Murthy NS, et al. Self-assembly and critical aggregation concentration measurements of ABA triblock copolymers with varying B block types:

- model development, prediction, and validation. *J Phys Chem B* 2016; **120**:3666–76.
107. Guan Z, Wang L, Lin J. Interaction pathways between plasma membrane and block copolymer micelles. *Biomacromolecules* 2017; **18**:797–807.
 108. You J, Hu FQ, Du YZ, Yuan H. Polymeric micelles with glycolipid-like structure and multiple hydrophobic domains for mediating molecular target delivery of paclitaxel. *Biomacromolecules* 2007; **8**:2450–6.
 109. Bertrand N, Grenier P, Mahmoudi M, Lima EM, Appel EA, Dormont F, et al. Mechanistic understanding of *in vivo* protein corona formation on polymeric nanoparticles and impact on pharmacokinetics. *Nat Commun* 2017; **8**:1–8.
 110. Gunawan C, Lim M, Marquis CP, Amal R. Nanoparticle–protein corona complexes govern the biological fates and functions of nanoparticles. *J Mater Chem B* 2014; **2**:2060–83.
 111. Papini E, Tavano R, Mancin F. Opsonins and dysopsonins of nanoparticles: facts, concepts, and methodological guidelines. *Front Immunol* 2020; **11**:2343.
 112. Karmali PP, Simberg D. Interactions of nanoparticles with plasma proteins: implication on clearance and toxicity of drug delivery systems. *Expet Opin Drug Deliv* 2011; **8**:343–57.
 113. Ogawara KI, Furumoto K, Nagayama S, Minato K, Higaki K, Kai T, et al. Pre-coating with serum albumin reduces receptor-mediated hepatic disposition of polystyrene nanosphere: implications for rational design of nanoparticles. *J Control Release* 2004; **100**:451–5.
 114. Kreuter J, Shamenkov D, Petrov V, Rameg P, Cychutek K, Koch-Brandt C, et al. Apolipoprotein-mediated transport of nanoparticle-bound drugs across the blood–brain barrier. *J Drug Target* 2002; **10**:317–25.
 115. de Castro CE, Panico K, Stangherlin LM, Ribeiro CA, da Silva MC, Carneiro-Ramos MS, et al. The protein corona conundrum: exploring the advantages and drawbacks of its presence around amphiphilic nanoparticles. *Bioconjugate Chem* 2020; **31**:2638–47.
 116. Zheng T, Jäättelä M, Liu B. pH gradient reversal fuels cancer progression. *Int J Biochem Cell Biol* 2020; **125**:105796.
 117. Tang H, Zhao W, Yu J, Li Y, Zhao C. Recent development of pH-responsive polymers for cancer nanomedicine. *Molecules* 2019; **24**:4.
 118. Ding HM, Ma YQ. Controlling cellular uptake of nanoparticles with pH-sensitive polymers. *Sci Rep* 2013; **3**:2804.
 119. Yang Y, Cai J, Zhuang X, Guo Z, Jing X, Chen X. pH-dependent self-assembly of amphiphilic poly(l-glutamic acid)-block-poly(lactic-co-glycolic acid) copolymers. *Polymer* 2010; **51**:2676–82.
 120. Mondal B, Pandey B, Parekh N, Panda S, Dutta T, Padhy A, et al. Amphiphilic mannose-6-phosphate glycopolymer-based bioactive and responsive self-assembled nanostructures for controlled and targeted lysosomal cargo delivery. *Biomater Sci* 2020; **8**:6322–36.
 121. Zhong XC, Xu WH, Wang ZT, Guo WW, Chen JJ, Guo NN, et al. Doxorubicin derivative loaded acetal-PEG-PCCL micelles for overcoming multidrug resistance in MCF-7/ADR cells. *Drug Dev Ind Pharm* 2019; **45**:1556–64.
 122. Momekova D, Ugrinova I, Slavkova M, Momekov G, Grancharov G, Gancheva V, et al. Superior proapoptotic activity of curcumin-loaded mixed block copolymer micelles with mitochondrial targeting properties. *Biomater Sci* 2018; **6**:3309–17.
 123. Chen Y, Feng X, Li L, Song K, Zhang L. Preparation and antitumor evaluation of hinokiflavone hybrid micelles with mitochondria targeted for lung adenocarcinoma treatment. *Drug Deliv* 2020; **27**:565–74.
 124. Debnath K, Jana NR, Jana NR. Designed polymer micelle for clearing amyloid protein aggregates via up-regulated autophagy. *ACS Biomater Sci Eng* 2018; **5**:390–401.
 125. Qu X, Zou Y, He C, Zhou Y, Jin Y, Deng Y, et al. Improved intestinal absorption of paclitaxel by mixed micelles self-assembled from vitamin E succinate-based amphiphilic polymers and their trans-cellular transport mechanism and intracellular trafficking routes. *Drug Deliv* 2018; **25**:210–25.
 126. Bathori G, Cervenak L, Karadi I. Caveolae—an alternative endocytotic pathway for targeted drug delivery. *Crit Rev Ther Drug Carrier Syst* 2004; **21**:67–95.
 127. Wang J, Byrne JD, Napier ME, DeSimone JM. More effective nanomedicines through particle design. *Small* 2011; **7**:1919–31.
 128. Chen D, Wang J, Wang Y, Zhang F, Dong X, Jiang L, et al. Promoting inter-/intra-cellular process of nanomedicine through its physicochemical properties optimization. *Curr Drug Metabol* 2018; **19**:75–82.
 129. Zhang Z, Qu Q, Li J, Zhou S. The effect of the hydrophilic/hydrophobic ratio of polymeric micelles on their endocytosis pathways into cells. *Macromol Biosci* 2013; **13**:789–98.
 130. Li Y, Yue T, Yang K, Zhang X. Molecular modeling of the relationship between nanoparticle shape anisotropy and endocytosis kinetics. *Biomaterials* 2012; **33**:4965–73.
 131. Shen Z, Ye H, Yi X, Li Y. Membrane wrapping efficiency of elastic nanoparticles during endocytosis: size and shape matter. *ACS Nano* 2018; **13**:215–28.
 132. Kozlov MM, McMahon HT, Chernomordik LV. Protein-driven membrane stresses in fusion and fission. *Trends Biochem Sci* 2010; **35**:699–706.
 133. Chen L, Xiao S, Zhu H, Wang L, Liang H. Shape-dependent internalization kinetics of nanoparticles by membranes. *Soft Matter* 2016; **12**:2632–41.
 134. Vácha R, Martínez-Veracoechea FJ, Frenkel D. Receptor-mediated endocytosis of nanoparticles of various shapes. *Nano Lett* 2011; **11**:5391–5.
 135. Morton SW, Herlihy KP, Shopsowitz KE, Deng ZJ, Chu KS, Bowerman CJ, et al. Scalable manufacture of built-to-order nanomedicine: spray-assisted layer-by-layer functionalization of print nanoparticles. *Adv Mater Technol* 2013; **25**:4707–13.
 136. Yi X, Gao H. Kinetics of receptor-mediated endocytosis of elastic nanoparticles. *Nanoscale* 2017; **9**:454–63.
 137. Kou L, Sun J, Zhai Y, He Z. The endocytosis and intracellular fate of nanomedicines: implication for rational design. *Asian J Pharm Sci* 2013; **8**:1–10.
 138. Haniu H, Saito N, Matsuda Y, Tsukahara T, Maruyama K, Usui Y, et al. Culture medium type affects endocytosis of multi-walled carbon nanotubes in BEAS-2B cells and subsequent biological response. *Toxicol Vitro* 2013; **27**:1679–85.
 139. Delva E, Jennings JM, Calkins CC, Kottke MD, Faundez V, Kowalczyk AP. Pemphigus vulgaris IgG-induced desmoglein-3 endocytosis and desmosomal disassembly are mediated by a clathrin- and dynamin-independent mechanism. *J Biol Chem* 2008; **283**:18303–13.
 140. Heuser JE, Anderson R. Hypertonic media inhibit receptor-mediated endocytosis by blocking clathrin-coated pit formation. *Int J Cell Biol* 1989; **108**:389–400.
 141. Carpentier JL, Sawano F, Geiger D, Gorden P, Perrelet A, Orci L. Potassium depletion and hypertonic medium reduce “non-coated” and clathrin-coated pit formation, as well as endocytosis through these two gates. *J Cell Physiol* 1989; **138**:519–26.
 142. Hansen SH, Sandvig K, Van Deurs B. Clathrin and HA2 adaptors: effects of potassium depletion, hypertonic medium, and cytosol acidification. *Int J Cell Biol* 1993; **121**:61–72.
 143. McAbee DD, Oka JA, Weigel PH. Loss of surface galactosyl receptor activity on isolated rat hepatocytes induced by monensin or chloroquine requires receptor internalization via a clathrin coated pit pathway. *Biochem Biophys Res Commun* 1989; **161**:261–6.
 144. Van Jaarsveld PP, Lippoldt RE, Nandi PK, Edelhoch H. Effects of several antimalarials and phenothiazine compounds on the formation of coat structure from clathrin. *Biochem Pharmacol* 1982; **31**:793–8.
 145. Lisanti Mp, Schook W, Moskowitz N, Beckenstein K, Bloom Ws, Ores C, et al. Brain clathrin: studies of its ultrastructural assemblies. *Eur J Biochem* 1982; **121**:617–22.
 146. Hertel C, Coulter SJ, Perkins JP. A comparison of catecholamine-induced internalization of beta-adrenergic receptors and receptor-mediated endocytosis of epidermal growth factor in human astrocytoma cells. Inhibition by phenylarsine oxide. *J Biol Chem* 1985; **260**:12547–53.

147. Rikihisa Y, Zhang Y, Park J. Inhibition of infection of macrophages with *Ehrlichia risticii* by cytochalasins, monodansylcadaverine, and taxol. *Infect Immun* 1994;**62**:5126–32.
148. Sargiacomo M, Sudol M, Tang Z, Lisanti MP. Signal transducing molecules and glycosyl-phosphatidylinositol-linked proteins form a caveolin-rich insoluble complex in MDCK cells. *J Cell Biol* 1993;**122**:789–807.
149. Schnitzer JE, Oh P, Pinney E, Allard J. Filipin-sensitive caveolae-mediated transport in endothelium: reduced transcytosis, scavenger endocytosis, and capillary permeability of select macromolecules. *J Cell Biol* 1994;**127**:1217–32.
150. Hooper NM. Detergent-insoluble glycosphingolipid/cholesterol-rich membrane domains, lipid rafts and caveolae. *Mol Membr Biol* 1999;**16**:145–56.
151. Dowrick P, Kenworthy P, McCann B, Warn R. Circular ruffle formation and closure lead to macropinocytosis in hepatocyte growth factor/scatter factor-treated cells. *Eur J Cell Biol* 1993;**61**:44–53.
152. Francis CL, Ryan TA, Jones BD, Smith SJ, Falkow S. Ruffles induced by *Salmonella* and other stimuli direct macropinocytosis of bacteria. *Nature* 1993;**364**:639–42.
153. Smith CM, Haucke V, McCluskey A, Robinson PJ, Chircop M. Inhibition of clathrin by pitstop 2 activates the spindle assembly checkpoint and induces cell death in dividing HeLa cancer cells. *Mol Cancer* 2013;**12**:4.
154. Goldenthal KL, Pastan I, Willingham MC. Initial steps in receptor-mediated endocytosis: the influence of temperature on the shape and distribution of plasma membrane clathrin-coated pits in cultured mammalian cells. *Exp Cell Res* 1984;**152**:558–64.
155. Araki N, Johnson MT, Swanson JA. A role for phosphoinositide 3-kinase in the completion of macropinocytosis and phagocytosis by macrophages. *Int J Cell Biol* 1996;**135**:1249–60.
156. Gschwendt M, Muller H, Kielbassa K, Zang R, Kittstein W, Rincke G, et al. Rottlerin, a novel protein kinase inhibitor. *Biochem Biophys Res Commun* 1994;**199**:93–8.
157. Rodal SK, Skretting G, Garred Ø, Vilhardt F, Van Deurs B, Sandvig K. Extraction of cholesterol with methyl- β -cyclodextrin perturbs formation of clathrin-coated endocytic vesicles. *Mol Biol Cell* 1999;**10**:961–74.
158. Orci L, Halban P, Amherdt M, Ravazzola M, Vassalli JD, Perrelet A. A clathrin-coated, Golgi-related compartment of the insulin secreting cell accumulates proinsulin in the presence of monensin. *Cell* 1984;**39**:39–47.
159. Cao J, Xie X, Lu A, He B, Chen Y, Gu Z, et al. Cellular internalization of doxorubicin loaded star-shaped micelles with hydrophilic zwitterionic sulfobetaine segments. *Biomaterials* 2014;**35**:4517–24.
160. Zheng C, Guo Q, Wu Z, Sun L, Zhang Z, Li C, et al. Amphiphilic glycopolymer nanoparticles as vehicles for nasal delivery of peptides and proteins. *Eur J Pharmaceut Sci* 2013;**49**:474–82.
161. Jiang X, Xin H, Ren Q, Gu J, Zhu L, Du F, et al. Nanoparticles of 2-deoxy-D-glucose functionalized poly(ethylene glycol)-co-poly(trimethylene carbonate) for dual-targeted drug delivery in glioma treatment. *Biomaterials* 2014;**35**:518–29.
162. Yang G, Wang J, Li D, Zhou S. Polyanhydride micelles with diverse morphologies for shape-regulated cellular internalization and blood circulation. *Regen Biomater* 2017;**4**:149–57.
163. Zhang W, Sun J, Liu Y, Tao M, Ai X, Su X, et al. PEG-stabilized bilayer nanodisks as carriers for doxorubicin delivery. *Mol Pharm* 2014;**11**:3279–90.
164. Xia H, Gao X, Gu G, Liu Z, Hu Q, Tu Y, et al. Penetratin-functionalized PEG–PLA nanoparticles for brain drug delivery. *Int J Pharm* 2012;**436**:840–50.
165. Zhou J, Chau Y. Different oligoarginine modifications alter endocytic pathways and subcellular trafficking of polymeric nanoparticles. *Biomater Sci* 2016;**4**:1462–72.
166. Starigazdová J, Nešporová K, Čepa M, Šínová R, Šmejkalová D, Huerta-Angeles G, et al. *In vitro* investigation of hyaluronan-based polymeric micelles for drug delivery into the skin: the internalization pathway. *Eur J Pharmaceut Sci* 2020;**143**:105168.